

## LIBRARY Michigan State University

This is to certify that the dissertation entitled

## MICROWAVE AND THERMALLY CURED NATURAL FIBER EPOXY COMPOSITES

presented by

### **NIKKI SGRICCIA**

has been accepted towards fulfillment of the requirements for the

Major Professor's Signature

Pecalum 9, 2008

Date

MSU is an Affirmative Action/Equal Opportunity Employer

PLACE IN RETURN BOX to remove this checkout from your record.

TO AVOID FINES return on or before date due.

MAY BE RECALLED with earlier due date if requested.

DATE DUE	DATE DUE	DATE DUE

5/08 K:/Proj/Acc&Pres/CIRC/DateDue.indd

# MICROWAVE AND THERMALLY CURED NATURAL FIBER EPOXY COMPOSITES

Ву

Nikki Sgriccia

## A DISSERTATION

Submitted to
Michigan State University
in partial fulfillment of the requirements
for the degree of

**DOCTOR OF PHILOSOPHY** 

**Chemical Engineering** 

2008

#### **ABSTRACT**

# MICROWAVE AND THERMALLY CURED NATURAL FIBER EPOXY COMPOSITES

By

## Nikki Sgriccia

Lignocellulosic natural fibers such as henequen, flax, hemp, and kenaf have many properties which make them an attractive alternative to traditional reinforcement materials such as glass, carbon, and aramid. In this study, research was performed in two sections. The first phase utilized conventional oven curing and single mode heating for microwave processing and untreated fibers for composite reinforcement material. Using this heating method, the size of the composites was restricted to very small samples. The second phase used variable frequency mode switching to cure larger samples with microwave heating. Fibers treated with alkali and silane were used in addition to untreated fibers. Modeling of the epoxy curing process was also conducted.

Single mode heating was used first to make small composite samples. These composites were examined using differential scanning calorimetry, dielectric testing, and thermogravimetric analysis. Untreated flax, henequen, hemp, and kenaf were used in this section of the study. Additionally, epoxy compatible glass was

used for comparison. Equivalent composites were also made with oven curing.

Variable frequency microwave heating utilizes complementary heating modes to cure larger composites. In this section, alkali and silane treatments were applied to kenaf and hemp fibers. The fibers and composites were examined using FTIR, XPS, water absorption testing, ESEM, and flexural testing. Following are some important findings from this research. Alkali treatment removes hemicellulose and lignin from fiber surfaces. Alkali treated hemp and kenaf composites absorb more water than other treated fiber composites. The silane treatment is effective in increasing the adhesion between the fiber and matrix.

Microwave processing of natural fiber composites has not been previously examined in literature. Natural fiber reinforced epoxy composites can be cured 75 minutes faster in the microwave than in the oven. The dielectric properties of natural fibers were studied and compared to the dielectric properties of glass fibers. It was found that the dielectric loss factors of all the fibers were similar, so all the fiber composites examined should interact with microwaves in a similar manner. This was confirmed with the DSC experiments. More work needs to be done on applying pressure to the natural and glass fiber reinforced composites to produce composites of higher quality using microwave curing.

Copyright by NIKKI SGRICCIA 2008

## Acknowledgements

I would like to thank my advisor Dr. Martin C. Hawley for his support during this research. I also appreciate the time and suggestions of my other committee members; Dr. Leo Kempel, Dr. Ramani Narayan, Dr. Krishnamurthy Jayaraman, and Dr. Greg Baker. I am also grateful to Mr. Mike Rich and Mr. Kelby Thayer for their training in equipment operation. Acknowledgement is also extended to Dr. Per Askeland for analyzing the surface of natural fibers with XPS. Finally, I would like to thank my parents, Bill and Mary Anne Sgriccia, for their unconditional love and support throughout my life. Without them, this dissertation would not have been possible.

## **TABLE OF CONTENTS**

LIST OF TABLES	viii
LIST OF FIGURES	ix
CHAPTER 1	
Introduction	
1.1 Problem Statement	
1.2 Approach	3
CHAPTER 2	•
Background	
2.1 Fibers	
2.2 Fiber Treatments	
2.3 Epoxy	
2.3.1 Epoxy Crosslinking	
2.3.2 Natural Fiber Composites	
2.3.3 Glass fiber Composites	
2.4 Conventional Curing	
2.5 Microwave Curing	
2.6 Material Characterization	
2.7 Summary	. 33
CHAPTER 3	
Experimental Methods and Results	35
3.1 Curing Studies	
3.2 Dielectric Testing	
3.3 Thermogravimetric Analysis	
3.4 Surface Treatments	47
3.5 Fourier Transform Infrared Spectroscopy	.48
3.6 X-Ray Photoelectron Spectroscopy	
3.7 Water Absorption	. 53
3.8 Environmental Scanning Electron Microscopy	
3.9 Fiber Selection	64
3.10 Curing Modes	
3.11 Composite preparation for mechanical property testing	68
3.12 Flexural Testing	
3.13 IR Analysis of Kenaf and Hemp Composites	71
CHAPTER 4	
Kinetic Modeling	. 75
4.1 Introduction	
4.2 Background	. 75
4.3 Kinetic Modeling Results	.81

CHAPTER 5 Discussion of Results	91
CHAPTER 6 Energy and Economics	97
CHAPTER 7 Conclusions	105
CHAPTER 8 Future Work	109
APPENDICES	113
REFERENCES	142

## LIST OF TABLES

Table 1: Composition of natural fibers	8
Table 2: Composition of E-Glass	9
Table 3: E-Glass Fiber Properties	. 10
Table 4: Degradation temperatures for glass and natural fiber composites	. 46
Table 5: Degradation temperatures for glass and natural fibers	.46
Table 6: Atomic concentration tables for treated and untreated fibers	52
Table 7: Fiber down selection table	64
Table 8: Summary of kinetic constants for neat epoxy and natural and glass fiber composites	
Table 9: Summary of hemp, kenaf, and glass properties	95
Table 10: Energy and economics for kenaf and glass	.102
Table 11: Economics for kenaf and glass composites	103

## LIST OF FIGURES

images in this dissertation are presented in color.	
Figure 1: Structure of cellulose	7
Figure 2: Structural model of lignin	7
Figure 3: Benzoyl chloride reaction	15
Figure 4: Acetylation reaction	15
Figure 5: Isocyanate reaction	17
Figure 6: Acrylonitrile reaction	18
Figure 7: Reaction of maleated-polypropylene with fibers	20
Figure 8: Structure of DGEBA	24
Figure 9: Circuit of the microwave curing system	.37
Figure 10: Scatter results for single-mode microwave cured DGEBA/DDS samples	39
Figure 11: Scatter results for oven cured samples	40
Figure 12: Curing results for microwave and conventionally processed glass and kenaf fiber reinforced composites	42
Figure 13: Dielectric constants of fibers and epoxy	43
Figure 14: Dielectric loss factors of fibers and epoxy	44
Figure 15: Spectrum of treated and untreated hemp fibers	.48
Figure 16: Spectrum of treated and untreated kenaf fibers	.49
Figure 17: Water absorption of natural and glass fiber composites (untreated)	54
Figure 18: Water absorption of natural and glass fiber composites (treated)	54
Figure 19: ESEM micrographs of fibers A) Kenaf B) Hemp C) Henequen D) Flax E) Glass	.58

Figure 20: Left: hemp. Right alkali treated hemp. Magnification 300 scale bar 150 μm5	
Figure 21: Top image: Untreated kenaf composite. Middle and bottom images: Silane treated kenaf composite. Scale bar 150 μm. Magnification 50x6	31
Figure 22: 3-glycidoxypropyltrimethoxysilane6	2
Figure 23: Silanization reaction6	3
Figure 24: Schematic of mold for flexural testing showing the location of the temperature probes6	6
Figure 25: Flexural Modulus for treated and untreated composites	9
Figure 26: ATR - FTIR Spectra of hemp and kenaf (untreated7	'2
Figure 27: Lignin monomeric unit7	'3
Figure 28: Cellulose monomeric unit7	'3
Figure 29: Epoxy curing mechanism	'6
Figure 30: Uncatalyzed and autocatalyzed epoxy curing reaction	
mechanisms 7	78
Figure 31: Curing curve for microwave cured hemp fiber composites	32
Figure 32: Curing curve for oven cured hemp fiber composites 8	32
Figure 33: Curing curve for microwave cured kenaf fiber composites	33
Figure 34: Curing curve for oven cured kenaf fiber composites 8	33
Figure 35: Curing curve for microwave cured glass fiber composites	34
Figure 36: Curing curve for oven cured glass fiber composites	34
Figure 37: Curing curve for microwave cured flax fiber composites	35

Figure 38: Curing curve for oven cured flax fiber composites85
Figure 39: Curing curve for microwave cured henequen fiber composites
Figure 40: Curing curve for oven cured henequen fiber composites
Figure 41: Curing curve for microwave cured neat epoxy87
Figure 42: Curing curve for oven cured neat epoxy87
Figure 43: Process flowchart for kenaf fiber production97
Figure 44: Process flowchart for glass fiber production
Figure 45: Flexural modulus comparison for kenaf101
Figure A1: A sample DSC plot of thermal transitions114
Figure B1: TE modes in an empty cavity with a diameter of
17.78 cm
Figure B2: TM modes in an empty cavity with a diameter of
17.78 cm137
Figure B3: Polarization mechanisms for water. The solid line represents the dielectric constant and the dashed line represents the dielectric loss factor
Figure B4: Absorbed power vs. frequency plot141

#### **CHAPTER 1: Introduction**

#### 1.1 Problem Statement

Glass and carbon fibers have proven to be the mainstay for many polymer composite reinforcements. Applications are many, including military and commercially significant applications such as fiberglass, carbon composite airframe structures, etc. Natural fibers are emerging as an attractive alternative to glass fibers in reinforced composites. Incentives for switching to natural fibers are their low cost, low density, acceptable specific mechanical properties, and biodegradability. Yet producing a viable composite material is not merely a question of mixing a little of this and a little of that into a polymer binder. There are important challenges that require scientific study. The main challenges of using natural fibers are low compatibility with matrix materials, low degradation temperatures, water absorption, and variation in mechanical properties. Often, these problems arise from the natural variability in the fiber stock used in the manufacture of the composite. There are economic and environmental reasons to move away from glass fiber reinforced petroleum based polymer composites to fully biodegradable natural fiber reinforced biopolymers such as cellulosic plastics, polylactides (PLA), starch plastics, and soy-based plastics. Today, bioplastics are not currently economically competitive with petroleum-based plastics. New materials made of natural fiber reinforced synthetic polymers combine the monetary and environmental benefits of natural fibers with the economic advantages of traditional synthetic polymers.

Typically, traditional convection ovens are used to process the composite part. This has the advantage of being relatively low-cost with the disadvantage of being relatively slow. Hence, although the set-up cost may be low, the actual cost-to-manufacture can be high. Microwaves have been studied as an alternative processing method for composites due to their beneficial effects on processing time, as well as mechanical and physical properties. Applications of this technology have been limited by the difficulty of achieving even and controlled heating, especially for relatively large samples. Microwave heating is volumetric, rapid, and selective; however, the non-uniform electromagnetic field strength in the microwave cavity and the exothermic heat of reaction of some matrix materials make temperature control challenging.

There is considerable interest in the field of natural fiber composites in structural applications, but little research has been done on microwave curing of these composites. The objective of this work is to develop high quality natural fiber epoxy composites, as a replacement for glass fiber composites, with reduced processing times using microwaves.

## 1.2 Approach

In order to create natural fiber composites for testing, first the fibers and polymer matrix were selected. Diglycidyl ether of bisphenol-A (DGEBA) cured with diaminodiphenyl sulfone (DDS) was chosen for the matrix. This epoxy was selected because it has been studied previously and information is available on curing studies and dielectric properties at different temperatures as well as on the kinetic modeling. DGEBA/DDS can be used as pipes, electrical insulation, adhesives, and protective coatings. Hemp, kenaf, henequen, and flax were selected because they are all grown in the United States. US auto makers are interested in these fibers because they can avoid the cost of transporting them from overseas. Glass fibers were selected for comparison because they are commonly used as fiber reinforcement in composites. Composites were produced using treated and untreated fibers. Silane and alkali were used to treat the natural fibers because studies showed that they increase fiber/matrix adhesion. Composites were processed using microwave and conventional thermal curing.

Creating high quality natural fiber composites requires several steps, each building upon the previous work. First, curing studies are performed with four types of natural fiber (kenaf, flax, hemp, and henequen) reinforced composites. The microwave cured natural fiber composites are compared to conventional thermally cured composites. Comparisons are also made to glass fiber reinforced

composites since these are commonly used in industry. These studies determine the effects of microwave processing on processing time and extent of cure. Differential scanning calorimetry (DSC) is used to determine the extent of cure. This step combined with additional tests to determine thermal stability and fiber/matrix adhesion is used to narrow the scope of this project to two types of natural fibers which are best suited to microwave processing. The curing reaction is modeled using a phenomenological model. The kinetic parameters are then determined using this model.

Since mechanical properties of composites are related to the compatibility of the fibers and matrix, modifiers are added to improve the fiber matrix interface. Alkali and silanes are used as modifiers since other research has been successful at improving composite properties with these modifiers by making the surface more rough and by bonding the fibers to the matrix.

The microstructure, thermal properties, and mechanical properties are characterized after each step to evaluate the progress of the experiments. Thermogravimetric analysis (TGA) is conducted to determine degradation temperatures. The dielectric constant and loss factor of the natural fibers are determined using dielectric tests. Experiments are also conducted to determine the water absorption and flexural strength. Environmental Scanning Electron Microscopy (ESEM) is used to examine the interfacial adhesion, morphology, and fracture dynamics of the composites. X-

ray Photoelectron Spectroscopy (XPS) is used to characterize the elemental composition of the fiber surfaces.

## **CHAPTER 2: Background**

The following literature review covers natural and glass fibers, fiber treatments, epoxy and natural fiber composites, epoxy crosslinking and conventional curing, polymer/microwave interactions, microwave curing, and material characterization.

### 2.1 Fibers

The following section covers natural and glass fibers and various methods of fiber modification. The natural fiber treatments, alkali and silane, used in this research were selected based on their ability to improve the fiber/matrix adhesion indicated by this review and on their low price and ready availability.

Lignocellulosic natural fibers such as hemp, henequen, flax, sisal, coir, banana fibers, jute, ramie, pineapple leaf (PALF), and kenaf have the potential to be used as a replacement for glass or other traditional reinforcement materials in composites. Cellulose, the main component of these fibers, is a polysaccharide made of anhydroglucose rings joined by a  $\beta$ -1,4 glycoside bond (Figure 1).

Figure 1: Structure of cellulose.

There are three hydroxyl groups per anhydroglucose ring which make the fibers hydrophilic. Moisture content of the fibers can be up to 12.6 wt% [1]. Natural fibers also contain lignin, hemicellulose, pectin, fats and waxes, water soluble components, and pigments [2]. See Figure 2 for the structure lignin.

Figure 2: Structural model of lignin.

See Table 1 for the composition of some natural fibers [1, 2]. Complete information on pectin, ash, fats, and waxes was not available for all fibers. Composition varies among the different types of fibers. This is due to origin age and retting [1].

Table 1: Composition of natural fibers [3].

Fiber Type	Cellulose %	Lignin %	Hemicellulose %	Pectin %	Ash %
Fiber Flax	71	2.2	18.6 - 20.6	2.3	
Kenaf	31 - 57	15 - 19	21.5 - 23		2 - 5
Hemp	57 - 77	3.7 - 13	14 - 22.4	0.9	
Henequen	77.6	13.1	4 - 8		

The natural fibers consist of cellulose fibrils cemented together by the middle lamella. The middle lamella consists of hemicelluloses, pectin, and waxes. Waxes can also be present on the fiber surface.

Natural fibers have many properties which make them an attractive alternative to traditional materials. They have high specific properties such as stiffness [4], impact resistance [5], flexibility [6], and modulus [7]. In addition, they are available in large amounts [8] and are renewable and biodegradable. Other desirable properties are low cost, low density, less equipment abrasion [6, 9], less skin and respiratory irritation [10], vibration damping [4, 5], and enhanced energy recovery [1, 10].

The hydrophilicity of natural fibers results in undesirably high moisture absorption and weak adhesion to hydrophobic matrices. Additionally, most natural fibers have low degradation temperatures (~200 °C) which make them incompatible with thermosets that have high curing temperatures. There are several other drawbacks to natural fibers such as variation in mechanical properties [5, 7], lower ultimate strength [9], lower elongation [9], problems with nozzle flow in injection molding machines [9], bubbles in the product [9], and poor resistance to weathering [11].

Hemp, kenaf, henequen, and flax were selected because they are all grown in the United States. US auto makers are interested in these fibers because they can avoid the cost of transporting them from overseas.

Glass fibers are commonly used as composite reinforcing material. The composition of E-Glass fibers is shown in Table 2 below [12].

Table 2: Composition of E-Glass

Composition	%
Silicon dioxide	52 - 56
Calcium oxide	16 - 25
Aluminum oxide	12 - 16
Boron oxide	8 - 13
Sodium and potassium oxides	0 - 1
Magnesium oxide	0 - 6

The structure of glass is a tetrahedron arrangement of silicon and oxygen where oxygen is often replaced by calcium, aluminum, or sodium [12]. Glass is selected as a reinforcement due to its desirable properties (see Table 3) and its low cost relative to aramid or carbon fibers [12, 13].

Table 3: E-Glass Fiber Properties

Properties	E-Glass
Specific gravity (g/cm <sup>3</sup> )	2.54
Tensile strength at 72 F (psi)	500,000
Yield strength at 1000 F (psi)	120,000
Modulus of elasticity 72 F (psi)	10,500,000
Elongation at 72 °F (%)	4.8
Coefficient of expansion (in/in/°F)	2.80E-06
Specific heat at 75 °F	0.192
Softening point (°F)	1555
Strain point (°F)	945
Annealing point (°F)	1215
Dielectric constant 72 °F	
Index of refraction	1.547

Other benefits of using glass fibers for composite reinforcement are consistent properties [1], ease of handling and molding [12], and low moisture absorption [12]. Glass fibers improve the impact properties, mechanical strength, dimensional stability, and range of useable temperatures over the matrix material [12]. Disadvantages of glass fibers include disposal at the end of the product life cycle [1], non-renewable resources required for production, high energy

consumption during production, abrasion of composite forming machines, and health hazards [13].

Glass fiber reinforced composites are commonly used in aircraft parts [12-17], sporting goods [13], filtration fabrics [12, 14, 15], rubber reinforcement [12, 16, 17], dental appliances [18-22], automotive parts [23-26], and other structural components [27].

#### 2.2 Fiber Treatments

Attempts to improve the bonding between natural fibers and matrix materials fall into two categories: increasing the physical linking and chemical bonding. Defatting and bleaching are used to increase physical linking while cyanoethylation, benzoylation, acetylation, coupling agents with isocyanate functional groups, and graft copolymerization are used to form bonds between the matrix and fibers. The effect of each treatment on the composite properties depended on the fiber matrix system used.

Most research has focused on fiber modification though some matrix modification was also attempted [9, 10]. Solution modification of fiber includes such treatments defatting [28-34]. as cyanoethylation [1, 30, 31, 35], bleaching [31, 35], benzoylation [6], acetylation [32, 35, 36], silanization [8, 29, 33], coupling agents with isocyanate functional groups [29, 37], plasma and copolymerization [28-30, 35, 38]. Treatments are often used in combination [35]. The results of these treatments varied with the matrix and reinforcement materials.

Defatting, or dewaxing, is sometimes the first step in fiber modification. One dewaxing process involves soaking the fibers in ethanol and benzene for several hours. Mishra et al. determined that defatting decreased the tensile strength of pineapple leaf fiber and polyester composites compared to untreated fiber composites [30]. This treatment was shown to increase the flexural strength and marginally increase the impact strength [30]. Mercerization, or NaOH treatment, was also used by several groups for dewaxing, often with other treatments [28-31, 35]. Fibers are treated with NaOH to remove lignin, pectin, waxy substances, and natural oils covering the surface of the fiber cell wall. This makes the surface of the fiber rough by revealing the fibrils [7]. Alkalization also changes the structure of cellulose from cellulose I to cellulose II [7]. Cellulose I and II are both crystalline with parallel and anti-parallel conformations in the unit cell [7]. Gulati and Sain studied the acidbase characteristics of hemp fibers [32]. They found that untreated hemp fibers were basic and alkali treated hemp fibers were more acidic. They also found that the alkali treatment improved the mechanical properties of the composites. Rodriguez et al. investigated the mechanical properties of alkali treated jute fibers in an epoxy vinyl ester resin [39]. They found that the alkali removed significant amounts of lignin and hemicellulose and possibly damaged the cell walls. This reduced the strength of the fibers causing a reduction in tensile strength and modulus. Pickering *et al.* studied alkali treated hemp fiber reinforced polypropylene and found that mechanical properties increased with the treatment [40]. They attributed this to an increase in packing density brought on by the removal of cellulose and lignin. Alkali treated ramie fibers showed a two to three fold increase in fracture strain over untreated fibers [41].

The effect of the alkali treatment, as well as other surface treatments, depends on the fiber and matrix used. Rout et al. reported that the alkali treatment was best for improving flexural strength, but not tensile strength, of coir and a biodegradable thermoplastic polyesteramide (trade name BAK) composite [31]. Coir is a coconut shell fiber. However sisal/BAK composites treated with sodium hydroxide had the highest tensile strength compared to other treatments and untreated fiber composites [35]. This same group showed the sisal/BAK composites to have a comparatively low increase in flexural strength compared to the control [35]. For sisal and low density polyethylene (LDPE), alkali was the least effective treatment for improving the tensile strength [28]. This was also the case for sisal and room temperature cured epoxy in terms of compressive strength and flexural strength, which decreased compared to the untreated composite [29]. For PALF/polyester composites, alkali treatment was better for tensile strength than defatted and cyanoethylated fibers but was less effective than cyanoethylated fibers for flexural and impact strength [30]. In the cyanoethylation surface treatment, the fibers are refluxed with acrylonitrile, acetone and pyridine then washed with acetic acid and acetone. This treatment improves the mechanical properties of the composites by chemically bonding the fiber to the polymer matrix [1]. This treatment was the best for increasing tensile strength of coir/BAK composites but was the worst for improving flexural strength [31]. For PALF and polyester resin, cyanoethylation was better than alkali treated or defatted fibers for improving flexural and impact strength [30]. This treatment was not a good choice for improving mechanical properties for sisal/BAK composites [35].

Fibers were bleached in sodium chlorite solution and then washed with sodium bisulfate. Bleached fiber coir/BAK and sisal/BAK composites had less tensile strength than their unmodified counterparts, due to loss of lignin [2, 31, 35]. Bleaching did improve the flexural strength over the unmodified composites which is attributed to the greater flexibility of the fibers after lignin is removed [31, 35].

Benzoylated fibers were soaked in sodium hydroxide, agitated in a benzoyl chloride and NaOH solution, and rinsed with ethanol. The benzoyl chloride forms an ester linkage to the fiber, reducing its hydrophilicity and making it more compatible with the matrix [6]. The

benzoyl chloride reaction with the fiber's cellulosic hydroxyl group is show below [3].

Fiber - O+ NaOH 
$$\longrightarrow$$
 Fiber - O-Na+ + H<sub>2</sub>O

Fiber - O-Na+ + CI  $\longrightarrow$  Fiber - O  $\longrightarrow$  + NaCI

Figure 3: Benzoyl chloride reaction

Benzoylation increased the tensile strength and modulus of polystyrene/sisal composites [6].

In the acetylation treatment, the fibers are first treated with NaOH, and then soaked in acetic acid followed by acetic anhydride [3].

Fiber + 
$$CH_3$$
 —  $C$  —  $CH_3$  — Fiber +  $CH_3COOH$  | OCHOCH<sub>3</sub>

Figure 4: Acetylation reaction.

Acetylation was the best for improving flexural strength of sisal/BAK composites. This was most likely due to the activated hydrogen atom on the acetyl carbon forming a bond with the BAK

[35]. This treatment also improved the tensile strength of these composites though other treatments were better [36].

In silane treatments, the silane in an organofunctional- or alkoxy-silane reacts with water to form silanol which then bonds with the hydroxyl groups on the fibers. The organofunctional groups can react with the matrix while alkoxy groups have Van der Waals interactions with the fiber. This was the most effective treatment for improving the compressive strength of sisal/epoxy composites [29]. With birch sawdust and polystyrene composites there was no significant improvement of mechanical properties, except for the modulus, with silane treatment [8]. It was suggested that the Van der Waals forces linking the fiber to the matrix were not strong enough to improve the properties [8]. Abdelmouleh et al. studied the effects of (3-methacryloyloxypropyl)trimethoxysilane, three silanes hexadecyltrimethoxysilane, and (3-mercaptoproyl)trimethoxysilane on alfa fibers and bleached pine [42]. They found that the silane treatments reduced water absorption by forming a dense linkage between the fibers and matrix thereby reducing the ability of the fibers to take up more water by expansion. Huda et al. investigated a silane-treated talc filler on recycled newspaper/polylactic acid composites [43]. They found that the storage modulus and tan  $\delta$ values were increased due to the better adhesion provided by the silane treatment.

The effectiveness of the coupling agents with isocyanate functional groups depends on the specific coupling agent used. Maldas *et al.* tested spruce sawdust fibers and polystyrene composites with three different isocyanates coupling agents: poly[methylene(poly(phenyl isocyanate)] (PMPPI), toluene 2,4-diisocyanate (TDI), and hexamethylene diisocyanate (HMDI). In all the cases, the NCO group in the coupling agent reacts with the OH group on the fiber constituents to form urethane bonds [8]. The reaction is shown below [3].

$$R \longrightarrow C \longrightarrow O + Fiber \longrightarrow OH \longrightarrow N \longrightarrow O \longrightarrow Fiber$$

Figure 5: Isocyanate reaction.

However the chemicals interact with the matrix in different ways. The PMPPI and TDI have electrons which interact strongly with polystyrene and PMPPI's polymeric nature ensures that the linking is continuous which made it the best treatment for improving mechanical properties [8]. The van der Waals forces which bind HMDI to the matrix make it an unfavorable fiber treatment compared to PMPPI and TDI [8, 37].

Graft copolymerization is another method used to improve the interaction between the matrix and the fibers. Maldas *et al.* used the xanthate method to graft styrene onto sawdust pulp [8]. A peroxide ferrous-ion system was used to initiate the grafting process. When completed, a soxhlet extraction was used to determine the grafting percentage. It was found that the mechanical properties of the grafted sawdust/polystyrene composite improved and were comparable to the isocyanate treatment also used in the study [8]. Methyl methacrylate (MMA) and acrylonitrile (AN) have also been grafted onto natural fibers to improve their compatibility [30, 31, 35]. The AN reaction is shown below [3].

Fiber — OH + CH<sub>2</sub> == CH — C == N 
$$\longrightarrow$$
 Fiber — O — CH<sub>2</sub> == CH — C == N Figure 6: Acrylonitrile reaction.

In these cases aqueous  $Cu^{2+}$  -  $IO_4^-$  initiated the grafting. Rout et al. tested both MMA and AN grafted coir/BAK fiber composites and determined that both showed improvements in tensile and flexural strength over the control with MMA showing more improvement than AN [31]. These increases were attributed to greater adhesion between the fibers and matrix. The elongation at break was reduced due to increased brittleness of the fibers. The results obtained by these studies depended on the percentage

grafted. There is a maximum percentage that can be used without reducing the effectiveness of the treatment.

In several experiments, matrix modification was also attempted to increase the compatibility between the fibers and the matrix [9, 10]. Karnani *et al.* used maleic anhydride treated polypropylene along with silane-treated kenaf fibers. The maleic anhydride was used in order to increase the polarity of the polypropylene. The reaction of natural fibers with maleic anhydride polypropylene is shown below [3].

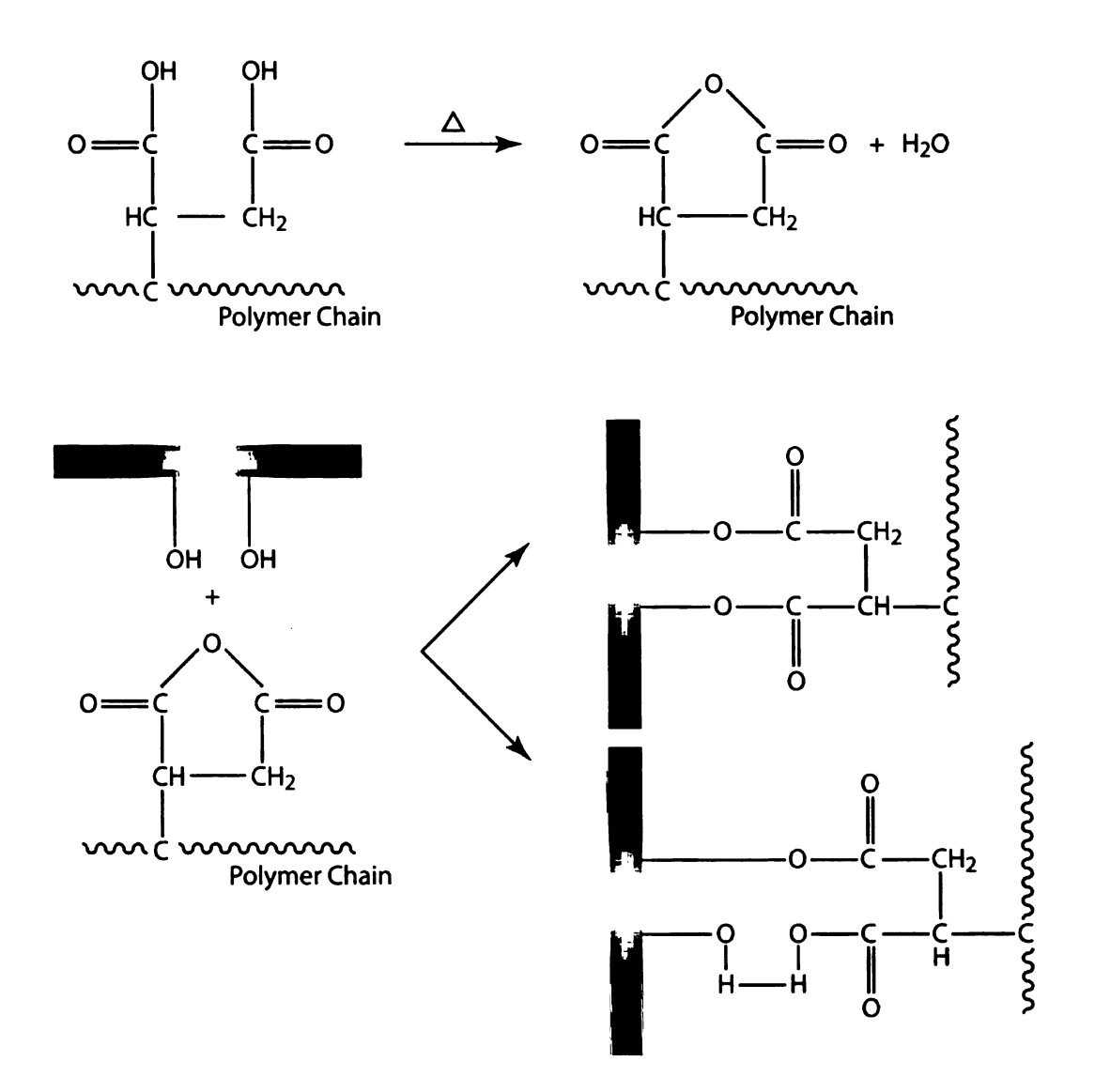


Figure 7: Reaction of maleated-polypropylene with fibers.

The result was increased tensile and flexural strength over the untreated composites and the fiber treated composites [10].

Grafting and other surface treatments can also improve the thermal stability and reduce moisture absorption of natural fibers. TGA analysis was used to show that the degradation temperature range shifted to higher temperatures with MMA and AN grafting, and benzoylation [6, 44, 45]. In the case of benzoylation, this shift is

attributed to the extraction of fiber components that degrade at lower temperatures or the restriction of fiber mobility due to bulky phenyl groups [6]. Surface treatments can reduce moisture absorption by increasing the hydrophobicity of the fibers. Sydenstricker *et al.* reported that moisture content in sisal fibers decreases with increasing concentrations of NaOH or N-isopropyl acrylamide with N-isopropyl acrylamide having the lowest content [5].

Alkali and silane were chosen for treating the natural fibers because they improved the adhesion between the fibers and matrix and are inexpensive and readily available. A thermoset epoxy was chosen because of the research group's prior experience with this material and availability of data.

Lee et al. studied the mechanical properties of untreated glass fiber mat/polypropylene composites [25]. They found that tensile and flexural modulus increased linearly with fiber content. The tensile and flexural strength peaked at 15 - 20% fiber content due to poor matrix-fiber adhesion and crack formation at fiber ends. Up to the optimum point, 15 - 20%, increasing fiber content also increased failure due to fiber pull-out, debonding, and plastic deformation.

Organofunctional silanes are commonly used to improve adhesion between glass fibers and polymer matrices. Several factors influence the effect of the silane treatment, including silane concentration, the effectiveness of bonding between the organofunctional group and the silane, the effectiveness of bonding between the silane and the glass, and the ability of the matrix material to diffuse into the transition zone between the matrix and the glass [46, 47]. The addition of 1 wt% silane coupling agent to glass/epoxy composites increased the bending performance of dental archwires [47]. Meric et al. studied the effect of [3-(methacryloyloxy)propyl] trimethoxysilane and two sizing agents, (linear polv(butvl methacrylate)) (PBMA) and crosslinking poly(methyl methacrylate) (PMMA) on PMMA composites [48]. The improved fiber/matrix adhesion was shown in SEM micrographs. Jancar studied E-glass treated with aminopropyltriethoxy silane and (3-methacryloyloxypropyl)trichloro silane in а polycarbonate composite [49]. The (3-methacryloyloxypropyl)trichloro silane had superior water absorption properties. Felix et al. studied polypropylene composites reinforced with vinyltriethoxysilane treated e-glass fibers [50]. The treated fibers increased fiber/matrix adhesion. Lower viscosity composites had better mechanical properties. Jensen et al. examined a hybrid sizing including two silanes. *n*-propyltrimethoxysilane (PTMO) 3and glycidoxypropyltrimethoxysilane (GPS) and colloidal silica [51]. This was compared to a compatible fiber sizing composed of 3glycidoxypropyltrimethoxysilane. The tensile strength of the hybrid treated glass fiber composites was greater than the compatible glass fiber treated composites. Pavlidou et al. studied glass fiber reinforced polyester composites with poly(dimethylsiloxane) added to improve adhesion [52]. These composites were compared to commercial silane treated glass fiber and untreated glass fiber composites. The interlaminar shear strength was greatest in the commercially treated glass fiber composites.

Other sizing agents such as a poly(vinyl acetate) film are also used to modify the glass fiber surface. These sizing agents can be used to protect the fiber surface from abrasion, minimize fiber breakage, and insulate the fibers from humidity [53]. Sizing agents and lubricants can reduce the effectiveness of coupling agents like silanes [53]. Alkali resistant glass fibers were coated with (3aminopropyl)triethoxysilane, epoxy film former and multi-walled carbon nanotubes and their mechanical properties were tested by Gao et al. [54]. They saw a fiber strength increase of 70% with only 0.2 wt% nanotubes due to roughness, thickness and coating modulus. Barazza et al. created admicellar-coated glass fibers in a EPON 815C matrix [55]. These composites had less water absorption than the uncoated fibers. Tanoglu et al. studied three glass fiber types, unsized, epoxy-compatible sized, and epoxy incompatible sized fibers [56]. The sizing contained the diglycidyl ether of bisphenol-A, a surfactant (an ethylene oxide and propylene oxide triblock silanes copolymer) and (glycidoxypropyltrimethoxysilane and methacryloxy propyl trimethoxy silane). The matrix was DGEBA (Shell Epon-828), cured with bis(4,4'-amino cyclohexyl) methane. The sizings were found to increase bonding and shear strength.

Sizing agents protect the surface of the glass fibers and also increase the adhesion between the glass fibers and the matrix material.

#### 2.3 Epoxy

The following sections cover epoxy crosslinking, natural fiber composites and glass fiber composites. DGEBA/DDS was selected as the epoxy for this study because it has been studied previously and information is available on curing studies and dielectric properties at different temperatures as well as on the kinetic modeling.

## 2.3.1 Epoxy Crosslinking

Epoxies can be used as the matrix in natural fiber composites (Figure 8).

Figure 8: Structure of DGEBA

Epoxy resins can be cross-linked with amines and anhydrides. The epoxide groups form bonds with the amine. Hydroxyl groups can also react with epoxides. The epoxide carbon which is attacked depends on the reaction conditions. The reaction product also contains hydroxyl groups, so the molecule can continue to react.

#### 2.3.2 Natural Fiber Composites

There has been a great deal of work done in the field of conventional processing of natural fiber composites. However, none of the current literature focused on microwave processing of natural fiber composites. Decreased curing time and volumetric curing are some of the potential benefits of microwave curing. Silane and alkali treatments were found to increase mechanical properties in some natural fiber composites which are why they were chosen for these experiments.

Since cellulose and lignin contain hydroxyl groups, natural fibers should bond to epoxide groups and become part of the network. O'Brien and Hartman used attenuated total reflectance (ATR) infrared spectroscopy to show that bonding takes place between reconstituted cellulose and epoxy [57]. The reaction is shown by a change in band intensities of key functional groups. The OH and C - O stretching bands of the cellulose, at 3350 and 1030 - 1055 cm<sup>-1</sup> respectively, decrease, while the symmetric and antisymmetric C-O stretching band, at 915 and 1160 cm<sup>-1</sup>,

disappear. The authors believe that cellulose is reacting with the unreacted epoxide groups in the system. Other groups also make reference to the bonding between natural fibers and an epoxy matrix [28, 58, 59]. Research on natural fiber and epoxy composites cured with conventional thermal processing has been conducted previously [28, 60, 61]. The work by Joseph and Rajulu was concerned with the effect of fiber content on mechanical properties [28, 61]. Oskman compared flax and glass fiber composites and found that glass and epoxy composites had larger tensile strength but smaller specific modulus [60].

Natural fibers can potentially bond to some matrix materials. However, it is not expected for their mechanical properties to match those of glass fiber composites because the properties of the natural fibers themselves are inferior to the glass fibers.

# 2.3.3 Glass Fiber Composites

Glass fiber reinforced epoxy composites have been extensively researched. Patel studied the mechanical and electrical properties of glass cloth reinforced DGEBA/phthalic anhydride [62]. The dielectric constant was approximately 3. Flexural strength ranged from 986 - 2447 kg cm<sup>-2</sup>. Tensile strength ranged from 895 - 1892 kg cm<sup>-2</sup> [62]. Kraynak et al. studied the effects of the application of vacuum at resin exit ports, mold temperature, initial resin temperature on the mechanical properties of glass fiber reinforced

epoxy composite [63]. The highest tensile strength was achieved with a mold temperature of 60°C (25, 40, 60, 80, 100, and 120°C were tested), an initial temperature of 28°C (15 and 28°C were tested), and with vacuum (0.03 bar) [63]. Composites made at atmospheric pressure had significantly lower mechanical properties [63]. Lee et al. modeled microwave curing of Fiberite S2/9134B epoxy reinforced with glass [64]. Their model provided the reflectance, transmittance, total absorbed energy, and absorbed energy distribution in the composite. Dielectric properties were tested and found to agree with their numerical model [64]. Abdel-Magid et al. examined the effects of mechanical loading and moisture conditioning on glass reinforced epoxy composites [65]. Composites gained strength at short durations and lost significant strength at long durations with moisture conditioning [65]. Composites exposed to mechanical loading and moisture conditioning simultaneously had a higher loss of strength [65].

Glass fiber reinforced epoxy composites have been researched for both microwave and conventional thermal curing. Use of vacuum during processing and lack of moisture during the usage phase provides better composite properties.

## 2.4. Conventional Curing

Typically, conventional ovens are used to cure epoxy composites. Conventional heating is a surface-driven, non-selective

process. The heat transfer coefficient of the composite's surface and the thermal conductivity of the composite controls the heating process. Heat is transferred from the surface of the composite to the interior during this process. This can cause temperature gradients in thick materials. Large temperature gradients cause residual stresses which decrease the mechanical properties of the composite. The curing cycle for poor thermal conductors, such as polymers, is long.

#### 2.5. Microwave Curing

Microwave heating shows promise for polymer and composites processing. Thermosets and thermoplastics have been studied in polymer processing. Microwave drying of thermoplastics has been investigated [66]. Microwave curing of thermosets have also been performed including polyesters [67], polyurethanes [68], polyimides [69] and epoxies [70-72]. Pulsed and continuous microwave curing of epoxies have been studied [72]. Batch [64] and continuous processes [72] have been studied in composites processing. Some results in microwave processing of polymers and composites include increased polymerization rate [69], reduced drying time for pelletized polycarbonate and polypropylene [66], increased Tg for cured epoxy [73], enhanced fiber/matrix adhesion in carbon composites [74]. and increased mechanical strength of graphite/epoxy composite [72]. Adhesive bonding studies have also been conducted [75, 76].

Microwave processing fundamentals can be more easily studied in a single mode resonant applicator as opposed to a multimode applicator. A single-mode applicator excites one mode at a time while a multi-mode applicator supports several modes at once. The electric field patterns inside the single mode applicator are easier to control and predict. In addition, single mode applicators are more efficient in coupling microwave energy into materials compared with multi-mode applicators [64].

In a single-mode applicator, uniform heating of large size materials can be achieved with mode-switching method. Fixed frequency mode switching has been used to process V-shaped polyester/glass composite parts [77]. In fixed frequency microwave processing, the cavity length is adjusted to accomplish mode switching. This process is slow and results in instability of temperature and non-uniform temperature distribution. Using a variable frequency microwave power source, polymers and composites were processed with microwaves with a variable frequency method [78]. This provided more uniform and stable processing of composite parts compared with fixed frequency mode switching.

In variable frequency curing, a numerical model is used to select resonant frequencies to cure a sample with an existing

microwave cavity or to design a microwave cavity to accomplish a desired processing task. The numerical model should include electromagnetic field distribution, microwave absorption, heat transfer, and chemical reactions. Dielectric permittivity and curing kinetics for polymers based on experimental data are required in the numerical model. The numerical results can be used to determine the temperature and curing profile in polymer sample, in addition to the electromagnetic field distribution within the microwave cavity [79]. The model can be used to develop control strategies to achieve more even curing. The energy balance for the microwave curing process within a volume of the material is shown below:

$$\rho C_p \frac{\partial T}{\partial t} = P + \nabla \cdot (\mathbf{k}(T) \cdot \nabla T) + \rho \frac{d\alpha}{dt} (-\Delta H_r)$$
 (2.1)

where  $\rho(\alpha)$  is density (kg/m³), P is the absorbed microwave power,  $C_p$  is heat capacity (J/kg/K), T is temperature (K), t is time (second), k is the anisotropic thermal conductivity tensor (W/K/m),  $\alpha$  is extent of cure, and  $-\Delta H_r$  is reaction heat (J/kg) [79]. The first term on the right accounts for EM heating while the second accounts for conduction. A convection boundary condition can be applied to the surface of the heated material.

$$-(\mathbf{k} \cdot \nabla T) \cdot \mathbf{n} = h(T - T_{\infty}) \tag{2.2}$$

The heat transfer, h, has units of  $kJ/m^2$ -s-°C. Typical values of h for heating or cooling air are 0.2 - 10  $kJ/m^2$ -s-°C [79]. A simplified equation for the reaction rate is:

$$\frac{d\alpha}{dt} = (1 - \alpha)^2 (k_1 + k_2 \alpha) \tag{2.3}$$

where  $\alpha$  is the extent of reaction, t is time,  $k_1 = e_0 K_1$ ' and  $k_2 = e_0^2 K_1$ ,  $e_0$  is the initial epoxide concentration,  $K_1 = A_1 e^{-E_1/(RT)}$  and  $K_1^{'} = A_1' e^{-E_1/(RT)}$  are specific reaction rate constants for the catalytic and noncatalytic reactions, respectively, R is the gas constant, T is the temperature,  $A_1$  and  $A_1$ ' are constants, and  $E_1$  and  $E_1$ ' are the activation energies [71]. The absorbed microwave power, obtained from the Poynting's Theorem, is:

$$P_{abs} = \int_{V} \frac{1}{2} \varepsilon \varepsilon \, \omega \, |\mathbf{E}| \, dV \tag{2.4}$$

where  $\epsilon''$  is the dielectric loss factor, E is the electric field vector inside the material (V/m),  $\omega$  is the frequency (rad/sec), and  $\epsilon_0$  is the free space permittivity [79]. The electric field, E, is the solution to the vector wave equation

$$\frac{\nabla \times \nabla \times \mathbf{E}}{\mu_r} - k_0^2 \varepsilon_r \mathbf{E} = 0 \tag{2.5}$$

where  $k_0$  is the free space wavenumber,  $\epsilon_r$  (F/m) is the free space permittivity, and  $\mu_r$  (H/m) is the free space permeability [79]. The propagation of electromagnetic fields happens on a much shorter time scale than thermal or composition effects. This allows the electromagnetic equations to be solved separately for power; this power is then used as an input for the coupled thermal and compositional equations. This model can be used to select the electric field patterns that can exist in a cavity which will also cure the desired sample. Mode switching may be required to cure large samples.

A simplified model is used to determine the curing mode used to cure the larger samples used in this research (see section 3.10).

#### 2.6. Material Characterization

Several experimental methods were used to characterize the natural and glass fiber composites and to evaluate the suitability of different natural fibers for composite applications. Differential scanning calorimetry was performed to determine the curing curve of the composites. Dielectric tests were performed to determine the dielectric properties of the fibers and the composites. Degradation

thermogravimetric analysis. Fourier transform infrared spectroscopy provides the spectra of the surfaces of treated and untreated fibers. X-ray photoelectron spectroscopy provides atomic concentrations on the surfaces of treated and untreated fibers. Water absorption tests determine the mass of water absorbed into composite samples over time. Environmental scanning electron microscopy was used to observe fiber surfaces and composite fracture surfaces. Flexural testing was performed to determine the flexural modulus of the natural fiber and glass fiber composites. The procedures used in these experiments are described in Appendix A.

## 2.7. Summary

Hemp, kenaf, henequen, and flax were selected because they are all grown in the United States. US auto makers are interested in these fibers because they can avoid the cost of transporting them from overseas. Alkali and silane were chosen for treating the natural fibers because they improved the adhesion between the fibers and matrix and they are inexpensive and readily available. Sizing agents protect the surface of the glass fibers and also increase the adhesion between the glass fibers and the matrix material. DGEBA/DDS was chosen because of the research group's prior experience with this material and availability of data and it is widely used in several applications. Microwave processing was selected

because it offers speed and energy saving advantages over conventional processing.

#### CHAPTER 3.0: Experimental Methods and Results

Chapter 1 described the advantages and disadvantages of using natural fibers for reinforcement of composite materials. Chapter 2 reviewed the literature on natural fiber composites and microwave heating fundamentals. This chapter applies single-mode and mode switching for microwave curing natural fiber and glass fiber composites. In single-mode curing, a single resonant frequency is used to cure small composites. Larger samples are cured by selecting two frequencies that have complimentary heating patterns and alternating them to achieve even heating. Curing studies (on both microwave and conventionally cured composites), dielectric testing, thermogravimetric analysis, surface treatments, Fourier transform infrared spectroscopy, x-ray photoelectron spectroscopy, water absorption, environmental scanning electron microscopy, curing modes, composite preparation, and flexural testing were performed and their results are discussed.

#### 3.1. Curing Studies

The natural fibers, kenaf, flax, industrial hemp, and henequen supplied, were soaked in hot distilled water for one hour, dried for 48 hours in air at room temperature, and dried in the oven at 100°C for 3 hours. The epoxy compatible chopped glass fibers were used as received.

Diglycidyl ether of bisphenol-A (DGEBA) cured with diaminodiphenyl sulfone (DDS) was used to produce the epoxy. The DGEBA was mixed with the DDS in the ratio of 2.79:1. Next 15 weight percent of fibers were mixed into the epoxy. The mixture was degassed in a 100°C vacuum oven for 20 minutes.

The amplified power signal in the microwave apparatus ranges from 0 to 200 Watts. Microwave frequency is adjustable from 2 GHz to 4 GHz manually or automatically. A 3-port circulator is used to prevent the reflected power from damaging the power source (see Figure 9). The input and reflected microwave powers are decoupled with 20db directional couplers (Narda 3043-20) and measured with power meters (HP435B). A dummy load is used to absorb most of the reflected power. A multi-channel LUXTRON fluoroptic thermometer and a multi-channel Nortech NoEMI-TS fiberoptic thermometer are used for sample temperature measurement. The probes are electrically nonconductive so they do not perturb or be perturbed by the microwave fields. The applicator was a Lambda Technologies Vari-wave Model 1000. The interior dimensions are 10" wide, 12" deep, and 10" high.

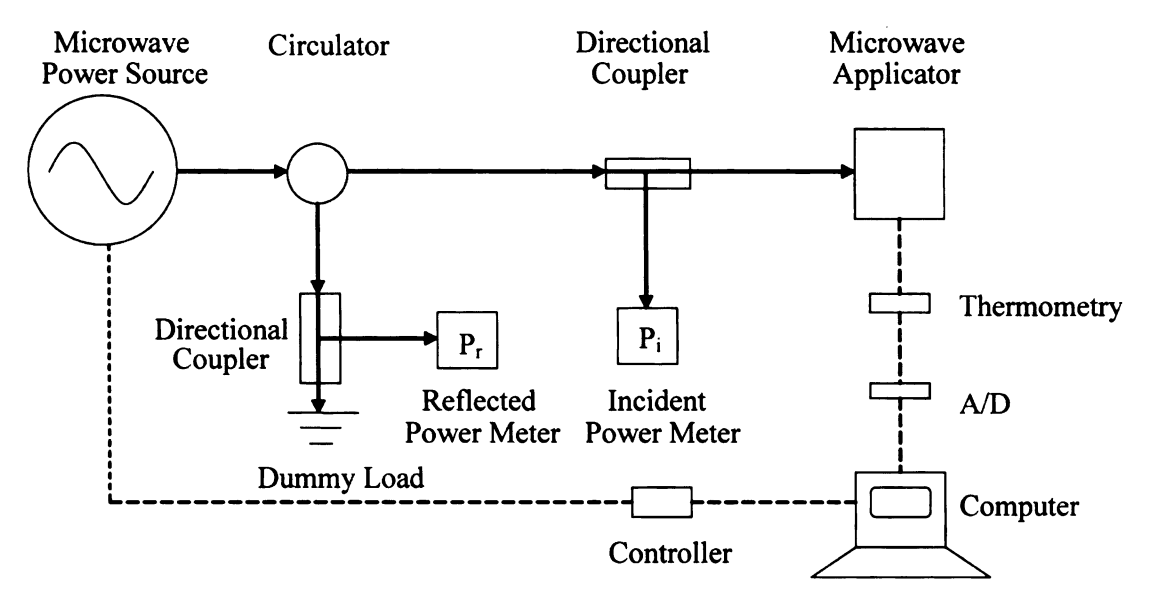


Figure 9: Circuit of the microwave curing system.

For the first phase, several grams of composite were placed in a cylindrical silicone rubber mold, 0.5 cm in diameter, and capped with a Teflon lid. In the second phase, a rectangular mold with holes for 6 samples of dimensions 3mm x 10mm x 15mm was used. An infrared temperature probe was inserted into the sample through the hole in the center of the Teflon lid. A heating mode was determined by frequency sweeping. A heating mode occurs when the reflected power is zero and the temperature rises quickly. Other modes, where the reflected power is zero, may be non-heating due to the shape of the EM field in the cavity. The temperature was controlled by changing the input power in the control program, LabView. The samples were then heated to 145°C in approximately 3 minutes.

Samples were held at the curing temperature for 20, 40, 60, 80, 100 and 120 minutes to develop an extent of cure vs. time curve (see section A.1.). Samples were also cured at the same temperature for the same durations in conventional oven for comparison.

The thermally cured samples are prepared from the same batch of material as the microwave cured samples. Several grams of composite were placed in a silicone rubber mold. The six samples are placed in the oven, without Teflon lids after the oven has reached 145°C. Samples were held at the curing temperature for 20, 40, 60, 80, 100 and 120 minutes to develop an extent of cure vs. time curve.

The differential scanning calorimetry was carried out in a TA Instruments DSC 2920. Ten samples, of 5-15 mg each, were tested for each composite, taken randomly throughout the sample. The sample was ramped to 350°C at 5°C/min then cooled with nitrogen to 40°C. Samples were cured in the single port microwave cavity and in a conventional oven from 20 minutes to 120 minutes. Plots of extent of cure vs. cure time show that there is more scatter present in the samples that were cured in the microwave than in oven cured samples (see Figures 10 and 11).

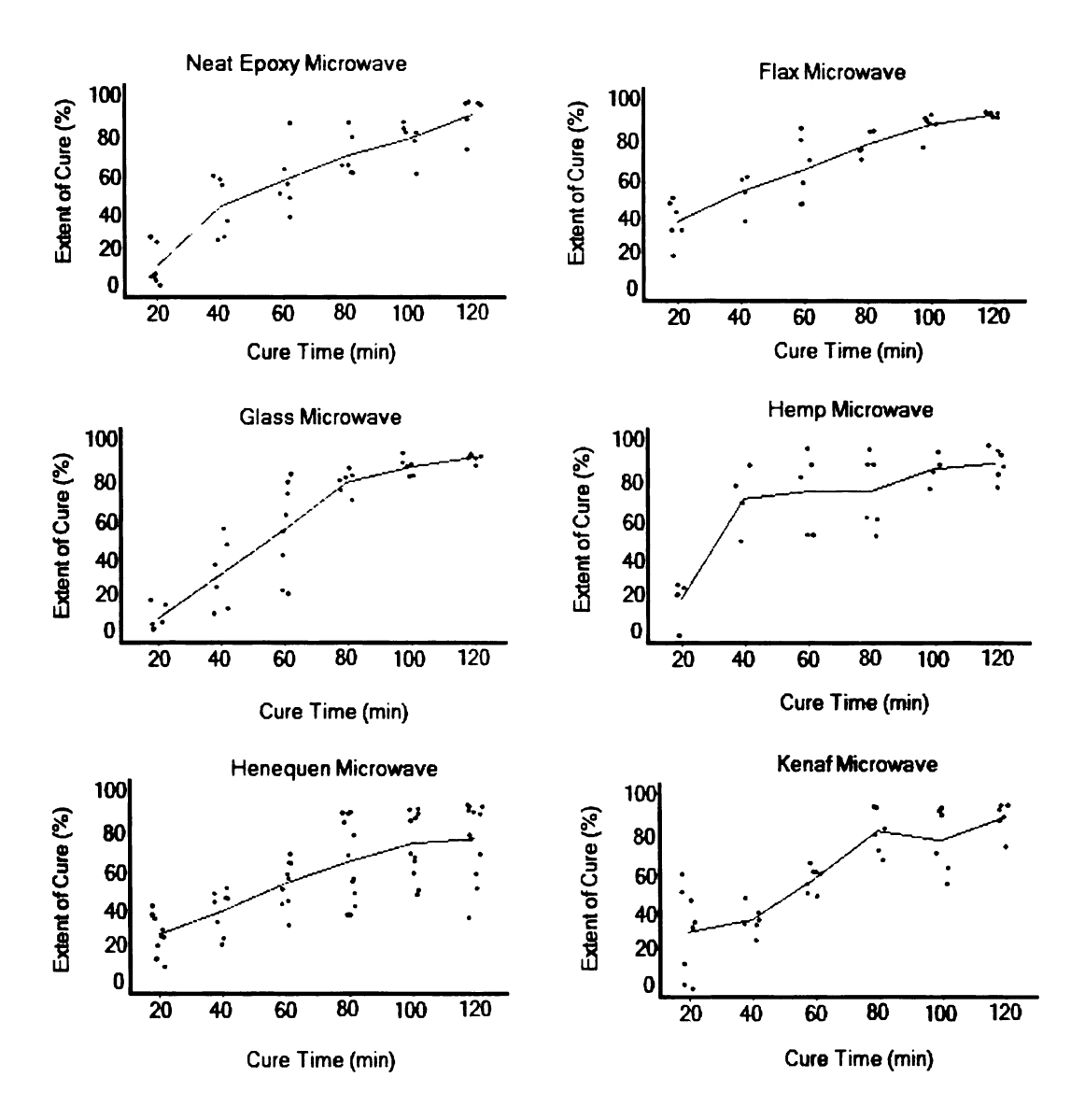


Figure 10: Scatter results for single-mode microwave cured DGEBA/DDS samples. The lines represent the average of the data points.

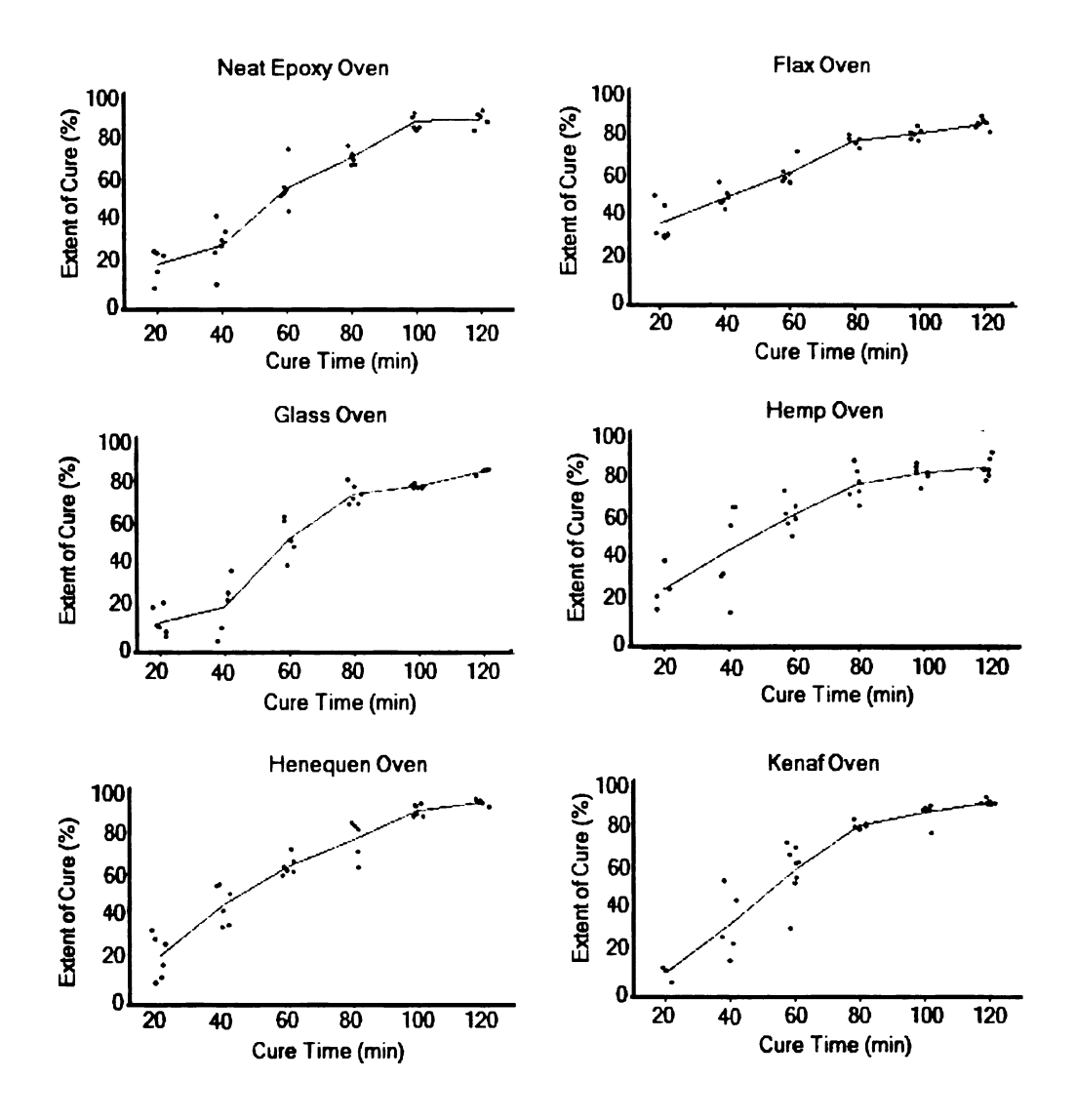


Figure 11: Scatter results for oven cured samples. The lines represent the average of the data points.

The scattering present in the microwave and oven cured composites is due to the sampling technique. For oven samples the curing is surface conduction limited so the center cures slower than the surface. Since the samples used for the DSC testing were from all throughout the composite, some samples will have a higher

extent of cure than others resulting in more scattering at short cure times. At long cure times, curing is more uniform and scattering decreases.

For the microwave curing, the mode pattern was center heating; therefore the surface of the microwave cured samples took longer to cure than the center. Consequently at shorter cure times, the surface was easy to cut with a razor blade and the DSC samples were all taken from there leading to less scattering. At long cure times, the samples were too hard to cut, so they were smashed like the oven samples. DSC samples were taken from all throughout the composite which may not have been evenly cured leading to more scattering at long cure times. The accuracy of the DSC machine itself is 2-4% so it is not primarily responsible for the scattering.

The microwave cured composites took 75 minutes less to reach the curing temperature (145°C). The figures are shown on the same time scale for comparison. The following figure shows the average extent of cure vs. time data for microwave and thermally cured glass and kenaf fiber reinforced epoxy composites. The natural and glass fiber composite curing curves were similar to each other and to neat epoxy. All the curves had the typical shape of autocatalytic reaction. This was expected from literature studies on the DGEBA/DDS matrix [79, 80].

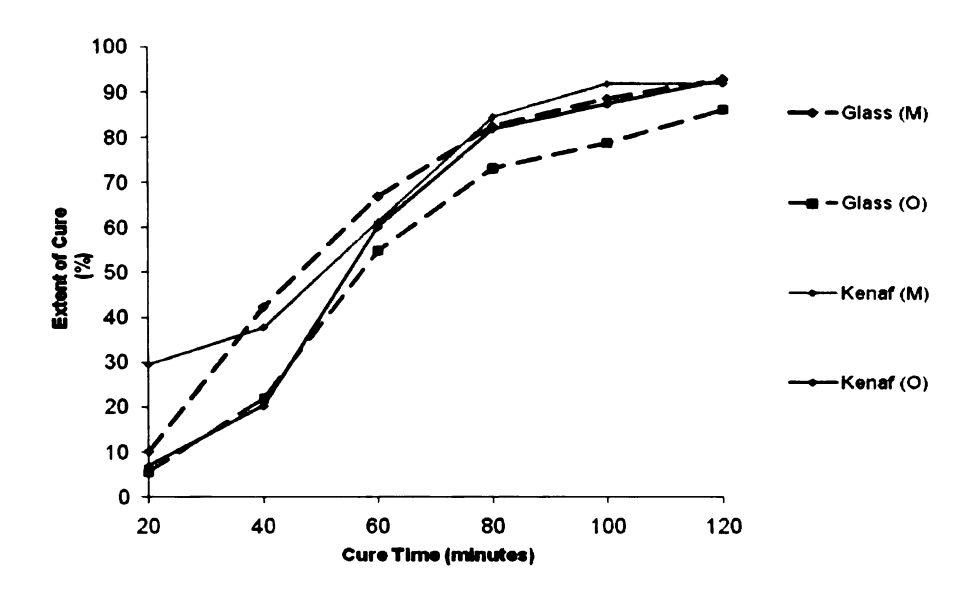


Figure 12: Curing results for microwave and conventionally processed glass and kenaf fiber reinforced composites, Data points represent the mean values.

In summary, the curing curves for neat epoxy, natural fiber composites, and glass fiber composites are similar. They have the typical shape of an autocatalytic reaction. The composites and neat epoxy reached an ultimate extent of cure of ~90% at 120 minutes. Microwave curing was 75 minutes faster overall than conventional thermal curing.

# 3.2. Dielectric Testing

Experiments were performed to determine the dielectric properties of the natural fibers, glass fibers, and composites because the propagation of microwaves through the materials depend on the dielectric properties (see section A.2). Fibers were prepared by washing in hot water, drying in air for 48 hours, and

oven drying for 3 hours. See Appendix A for the fiber preparation procedure. The fibers were then placed in a small Teflon holder and compressed. The compressed fibers were placed in an oven at 100°C until tested in the microwave cavity to ensure that the fibers contained as little moisture as possible.

Figures 13 and 14 show the dielectric constant and loss factor for natural and glass fibers and cured and uncured DGEBA/DDS.

Ten samples were averaged for each data point. The cavity method dielectric properties are measured at 2.45 GHz.

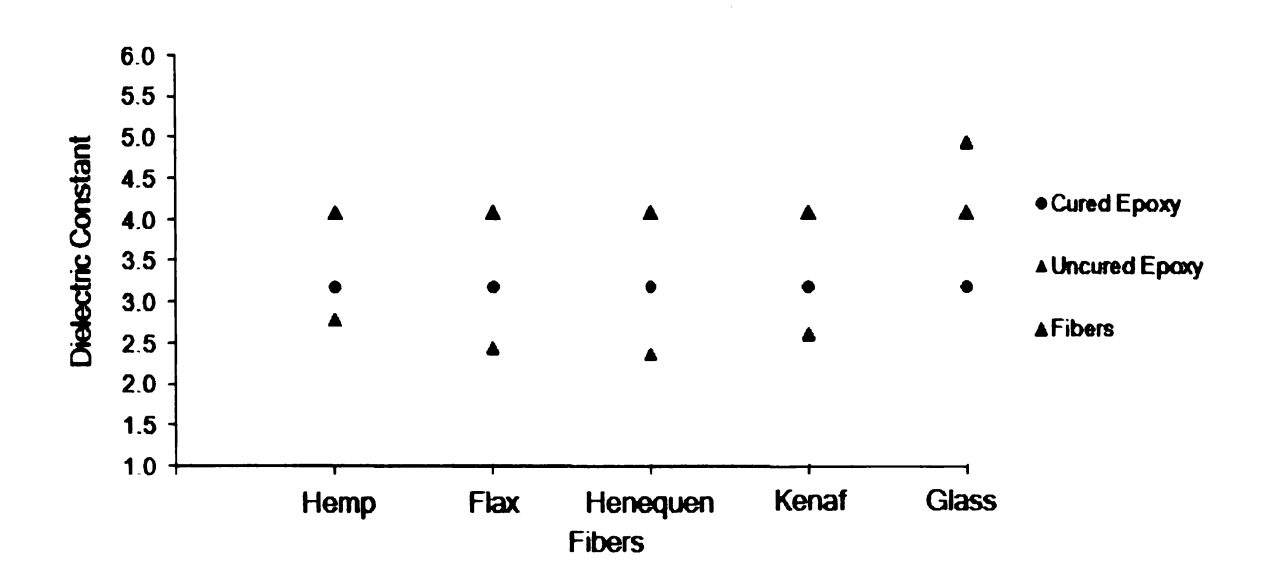


Figure 13: Dielectric constants of fibers and epoxy.

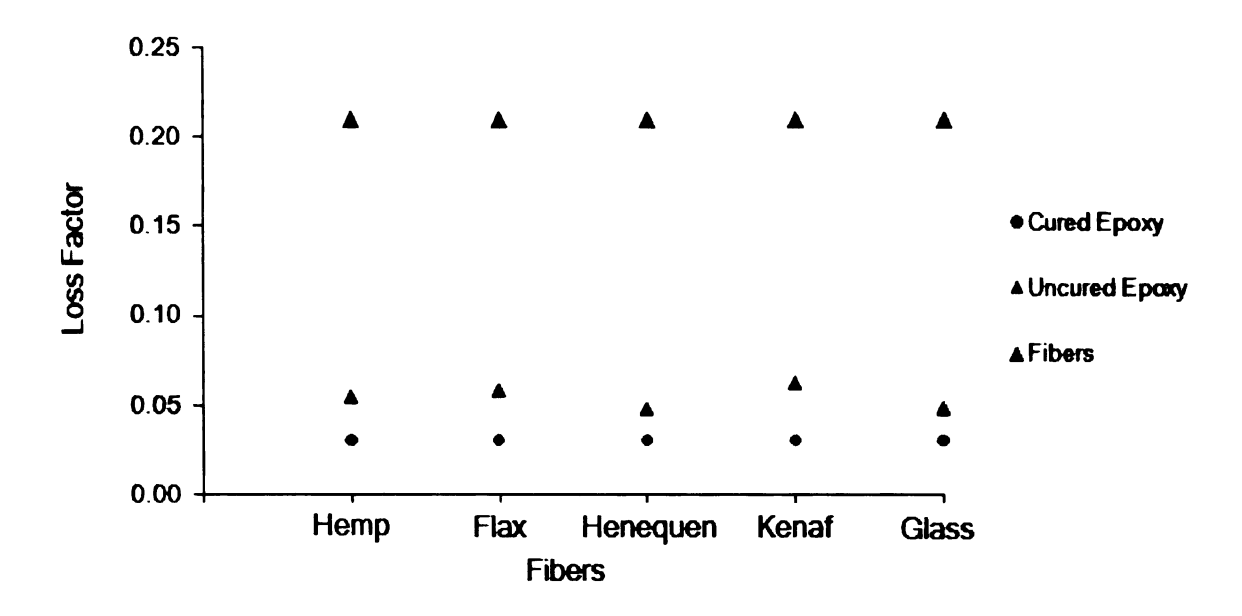


Figure 14: Dielectric loss factors of fibers and epoxy.

The dielectric constant characterizes the response of the material to the electric field. The dielectric constants were similar for the natural fibers. The dielectric loss factor indicates the material's ability to store energy. Since the uncured epoxy has a larger loss factor than the natural fibers, the microwaves will primarily heat the epoxy as the curing begins. As curing continues the dielectric loss factor of the epoxy decreases until it drops to a smaller value than that of the fibers. At that point the microwaves primarily heat the fibers. The natural and glass have similar loss factors.

See section A.2 for more information on the cavity and method procedure. See Figure B1 for variations in dielectric properties with frequency. The dielectric testing was conducted at 2.45 GHz. The natural and glass fibers had similar loss factors. The natural fibers

have the similar dielectric constant and the dielectric constant of the glass fibers is twice as large.

#### 3.3. Thermogravimetric Analysis

The thermogravimetric analysis of hemp, henequen, kenaf, flax and glass fibers and their composites was carried out in a TA Instruments Hi-Res TGA 2950 that was fitted to a nitrogen purge gas (see section A.3) to determine the degradation temperatures. The sample was conducted from ambient temperature to 600°C at 25°C/min. Mass is recorded as a function of temperature over the duration of the experiment. The initial weight loss at low temperatures is attributed to loss of absorbed moisture on the natural fibers. Degradation that does not result in a weight loss is not accounted for by this experiment.

Degradation temperatures of natural fiber composites (microwave and thermally cured) are lower than neat epoxy or glass fiber composites (see Table 4). This was also seen in literature [81, 82].

Table 4: Degradation Temperatures for Glass and Natural Fiber Composites

Composites	T (°C) 5%	T (°C) 25%	T (°C) 50%	T (°C) 75%	
Glass oven	400	N/A	402	539	
Glass microwave	400	N/A	402	482	
Hemp oven	348	384	392	472	
Hemp microwave	352	390	393	474	
Flax oven	364	389	393	474	
Flax microwave	351	385	391	472	
Kenaf oven	321	371	390	479	
Kenaf microwave	336	382	392	479	
Henequen oven	306	375	391	456	
Henequen microwave	355	389	392	483	
Neat Epoxy oven	397	N/A	398	490	
Neat Epoxy microwave	403	N/A	N/A	484	

All of the DGEBA/DDS composites have less than 5% weight loss at the curing temperature (145°C).

Table 5: Degradation temperatures for glass and natural fibers. Note: \* indicates the ultimate weight loss was 1.6%

Fibers	T (°C) 5%	T (°C) 25%	T (°C) 50%	T (°C) 75%	
Hemp	105	329	341	458	
Flax	88	323	339	441	
Kenaf	64	313	341	371	
Henequen	61	301	337	392	
Glass *	586				

Hemp has the highest degradation temperature of the natural fibers.

Glass fibers do not degrade at the curing temperature.

#### 3.4 Surface Treatments

The alkali and silane treatments were selected because the literature survey indicated that they improved fiber/matrix adhesion and they are readily available and inexpensive (see section A.4).

Fibers were treated using 2.25 mol% solution of sodium hydroxide [36]. The fibers were submerged in the sodium hydroxide solution for one hour at room temperature, rinsed with tap water, and then neutralized in a 2 vol% glacial acetic acid and tap water solution. The fibers were then rinsed with deionized water and dried at room temperature for 24 hours.

Fibers were treated using a one percent solution of (3-glycidoxypropyl)trimethoxysilane (Z-6040 from DOW Corning) in deionized water and ethanol in a 1:1 volume ratio [33]. This silane was chosen because it has an epoxide group at one end that can bond with the polymer matrix and alkoxy groups at the other end that have van der Walls interactions with the fibers. The pH of this solution was adjusted to 4 using 2% glacial acetic acid. The solution was stirred for two hours before the fibers were added. The fibers were washed with deionized water after the silane treatment. The fibers were then dried for 12 hours in air and then cured in a convection oven for five hours. After the fibers were treated, they were used to reinforce the DGEBA/DDS composites and were tested using FTIR, XPS, water absorption, ESEM, and flexural testing.

#### 3.5 Fourier Transform Infrared Spectroscopy

FTIR identifies the frequencies of vibrations of the bonds between atoms in a molecule by recording the molecular absorbance of infrared light. FTIR was preformed to gain information on the effects of the alkali and silane treatment on the natural fibers.

Kenaf and hemp fibers were analyzed before and after alkali and silane treatment using a Perkin Elmer Instruments Spectrum One with the Attenuated Total Reflectance (ATR) technique (see section A.5). The spectrum was shifted to set the absorbance equal to zero at 3323 cm<sup>-1</sup> (see Figures 15 and 16).

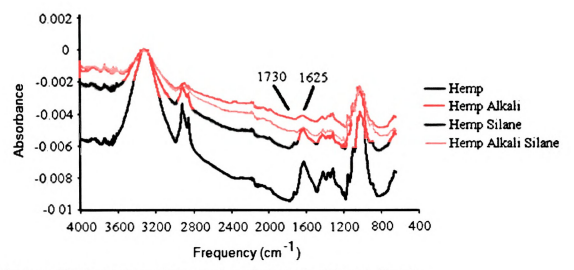


Figure 15: Spectrum of treated and untreated hemp fibers.

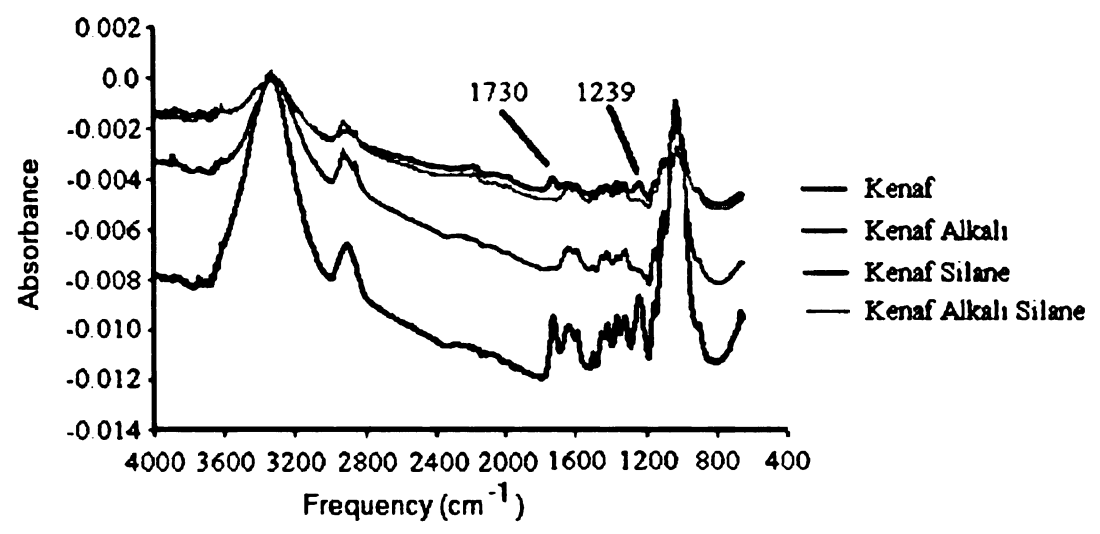


Figure 16: Spectrum of treated and untreated kenaf fibers.

The effects of fiber treatment on the natural fiber surfaces were also studied using FTIR. The peak 1730 cm<sup>-1</sup> is attributed to the C-O stretching on hemicellulose [83, 84]. This peak is not present in the alkali treated samples. The removal of hemicellulose from the fiber surfaces causes this peak to disappear [84]. The peak at 1239 cm<sup>-1</sup> in the kenaf fibers is much smaller for alkali treated samples. This peak is a C-O stretch of the acetyl group of lignin and is reduced because lignin is partially removed from the fiber surface [84]. The peak at 1625 cm<sup>-1</sup> is reduced in hemp alkali treated fibers and removed in kenaf alkali treated fibers. This peak represents the C=O bonds on hemicellulose and is further evidence that hemicellulose is removed from fiber surfaces by the alkali treatment [85]. FTIR does not show the presence of silane on the fibers. Peaks should be present at 766 cm<sup>-1</sup> and 847 cm<sup>-1</sup> [86]. It is possible that

the concentration of silane on the fiber surfaces is too small to detect by FTIR.

The FTIR experiments indicated that hemicelluloses and lignin are partially removed by the alkali treatment which is consistent with the literature review.

#### 3.6 X-Ray Photoelectron Spectroscopy

Untreated hemp, henequen, flax, and kenaf were tested using XPS in addition to alkali and silane treated hemp and kenaf. This was done to determine the elemental composition of the fiber surfaces. This was important for studying the fiber matrix adhesion.

XPS was performed with Physical Electronics PHI 5400 ESCA system, with a non-monochromatic Mg source operating at 300W (see section A.6). The spot size of the analyzer was 250  $\mu$ m<sup>2</sup> and the operating pressure was approximately 3.386 x 10<sup>-4</sup> Pa. The samples were mounted onto a stainless steel stub using a Mo mask. The take off angle was 45 degrees.

The spectra for all fibers (see Table 6) contained carbon and oxygen, while nitrogen, calcium, silicon and aluminum were detected in some samples. Cellulose, hemicellulose and pectin have an O/C ratio of 0.83 while lignin has a ratio of 0.35. Since the O/C of treated and untreated fibers in Table 6 is less than 0.83 the surface must have a large proportion of lignin and waxes [87, 88]. Natural fibers were dried at 100°C to reduce moisture prior to XPS testing. Out of

the four types of untreated natural fibers, Kenaf had the highest O/C ratio and flax had the lowest. The O/C ratio of treated kenaf fibers was larger than their hemp counterparts.

XPS testing showed that the fiber surface has more lignin (than cellulose), which helps bond the cellulose fibrils together, and waxes, which can act as a barrier. The treated and untreated kenaf fibers had more surface lignin and waxes than their hemp counterparts.

Table 6: Atomic concentration tables for treated and untreated fibers.

		_	63.84				7.55		0.38
		Henednen	78.27	1.87	19.55	0.31			0.25
		Flax	83.88		16.12				0.19
Silane/alkali	treated	kenaf	49.89	2.13	40.38	0.51	7.09		0.81
		kenaf	64.83	2.1	27.9	0.18	3.33	1.65	0.43
Silane	treated	kenaf	63.67	3.65	27.68		2.84	2.15	0.43
			62.34					2.76	0.45
	Silane/alkali	treated hemp	.13 78.49	2.81	18.15	0.26	0.28		0.23
Alkali	treated	hemp	83.13	1.84 48.	14.44		0.59		0.17
		hemp	71.75	3.45	23.03	0.61	1.16		0.32
		Hemb	76.79	2.19	20.48	0.53			0.27
			C (1s)	N (1s)	O (1s)	Ca (2p)	Si (2p)	AI (2p)	2/0

#### 3.7 Water Absorption

Water absorption experiments were conducted because the absorption of water can cause changes in the shape, debonding, or loss of strength in products regularly exposed to moisture [88]. Composites reinforced with hemp, glass, flax, kenaf, and henequen were tested. Also, alkali treated and silane treated kenaf and hemp reinforced composites were tested. The epoxy used was DGEBA/DDS. All composites were cured in the oven.

Composites with dimensions 25.4 mm x 38.1 mm x 3 mm were immersed in distilled water (see section A.7). Before taking weight measurements, the composite surfaces were blotted with paper towels to remove surface water. Measurements were taken at 6, 24, 48, 72, and 144 h for untreated samples. The weight was then measured weekly until the composites were saturated. The treated samples were weighed at 5, 24, 48, 120, and 168 h and thereafter weighed weekly until saturated.

Untreated henequen composites absorbed the most water (see Figures 17 and 18). There were ten samples tested per data point and the error bars represent the standard deviation.

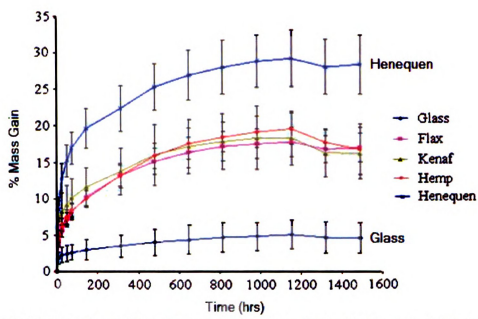


Figure 17: Water absorption of natural and glass fiber composites (untreated).

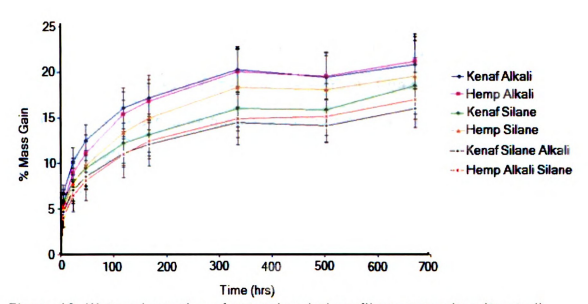


Figure 18: Water absorption of natural and glass fiber composites (treated).

Glass composites absorbed the least amount of water. Henequen composites absorbed water most quickly followed by kenaf, hemp and flax, and glass composites in the short run. Over the long term, flax, kenaf and hemp all have similar absorption

rates. Henequen, flax, kenaf, and hemp composites reached saturation at 816 h while glass composites reached saturation at 648 h. The henequen reinforced composites absorbed twice as much water as the other natural fibers.

The alkali treated kenaf and hemp composites absorb more water than the silane only or alkali and silane treated composites. The alkali and silane treated composites absorbed the least amount of water. Kenaf composites absorbed less water overall than their hemp counterparts. The silane treated, alkali and silane treated, and untreated composites had similar water absorption profiles.

These experiments show that the untreated and treated natural fiber composites absorb significantly more water than the glass fiber composites. This was expected as natural fiber composites absorb water in the fibers and matrix and water also exists in the voids of the composite. While in glass fiber composites, water is not absorbed into the fibers. Olmos *et al.* conducted experiments on silane treated glass fiber composites (25 wt%) and obtained a saturation mass gain of 4.21 - 5.22% depending on the treatment [89]. The untreated natural fibers in our experiments had 4.6% mass gain. The rate of water absorption in our samples is consistent with those in the treated fiber experiments. Williams and Wool tested composites made using plant oil based resins and flax fibers (30 wt%) [90]. The saturation weight for these composites ranged from 10.4 to 12.4%. Tserki *et al.* made 30 wt% flax and polyester

composites with a saturation mass gain of approximately 6.5% [88]. Our flax fiber and epoxy composites had a saturation mass gain of 17.2%. Tserki et al. made 30 wt% hemp polyester composites with a saturation mass gain of ~6% [88]. The hemp epoxy samples in these experiments reached 18.4% mass gain. Tajvidi et al. conducted experiments on 25 wt% kenaf polypropylene composites which had a saturation mass gain of around 2% [91]. The kenaf epoxy samples in these experiments reached 17.8% mass gain at saturation. Differences between these results and literature results can be attributed to different fiber loading and matrix composition and possibly due to voids present in our composite samples. In Figure 19 and 26, it can be seen that the alkali treated composites absorb more water than the untreated or silane treated composites. Fibers are treated with NaOH to remove lignin, pectin, waxy substances, and natural oils covering the surface of the fiber cell wall. makes the surface of the fiber rough by revealing the fibrils [85]. This change in fiber morphology may create more voids for water to absorb into.

The alkali treatment was a good treatment for cleaning the surface of the natural fibers but had a detrimental effect on water absorption. The henequen fibers were not selected for fiber treatment due to their poor performance in the water absorption experiments.

#### 3.8. Environmental Scanning Electron Microscopy

Untreated and alkali and silane treated natural fibers and glass fibers as well as treated and untreated fiber composites were examined using ESEM to view the effects of the fiber treatments on the fiber surfaces and composites. Adhesion of matrix material to fibers at the fracture surface will be visible.

The samples were observed in Philips ElectroScan 2020 ESEM (see section A.8). The sample chamber pressure was reduced to approximately 4.4 Torr. The working distance ranged from 6 - 9 mm. The focus, contrast, brightness and magnification were adjusted to provide the best image. The ESEM images were taken of the samples used for DSC analysis and flexural testing (see Figures 19 - 21).

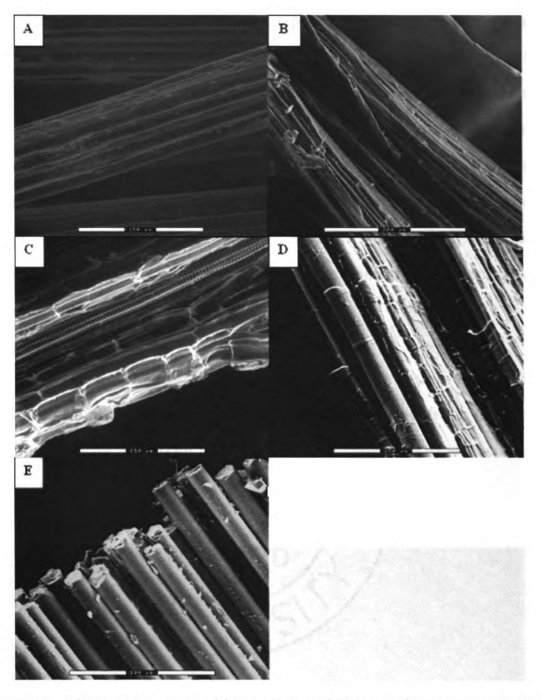


Figure 19: ESEM micrographs of fibers A) Kenaf B) Hemp C) Henequen D) Flax E) Glass. Scale bar is 150  $\mu m.$ 

Natural fibers form circular or polygonal bundles of ultimates bound together by the middle lamella. Glass fibers are cylindrical and the bundles are relatively flat. Kenaf forms short, polygonal fibers with a striated surface [92]. Hemp fibers are generally longer than kenaf, polygonal, and have an irregular surface [92]. Henequen fibers have a cross section that changes from beamlike to round along the fiber length with a smooth, straight surface [92]. Flax fiber surfaces are smooth. Flax fibers have a polygonal cross section and are short and non-continuous [93].

The ESEM image in Figure 20 shows that the interfibrillar material, hemicellulose and lignin, is etched away from the hemp fiber surface by the alkali treatment. Kenaf (not shown) was similarly affected.

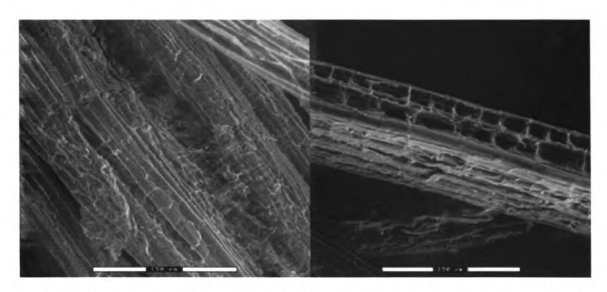


Figure 20: Left: hemp. Right alkali treated hemp. Magnification 300x, scale bar 150  $\mu\text{m}.$ 

The top image in Figure 21 shows a clean fiber pulled out at the kenaf composite fracture surface. The middle image shows a silane treated kenaf composite fracture surface. The fiber bundle shown is coated in epoxy. The bottom figure shows the top of the fiber bundle with the fibers exposed. These images show that the silane treatment was effective in increasing the fiber/matrix adhesion.

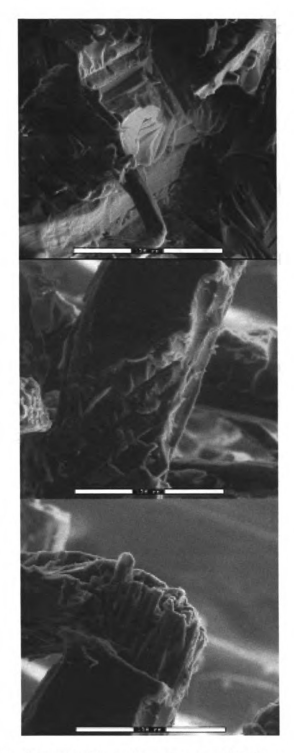


Figure 21: Top image: Untreated kenaf composite. Middle and bottom images: Silane treated kenaf composite. Scale bar 150  $\mu m$ . Magnification 350x.

The silane used in this case was (3-glycidoxypropyl) trimethoxysilane (Z-6040 from DOW Corning) an organofunctional

silane (Figure 22). This silane was chosen because its epoxide groups will react with the curing agent (DDS) and become part of the crosslinked network.

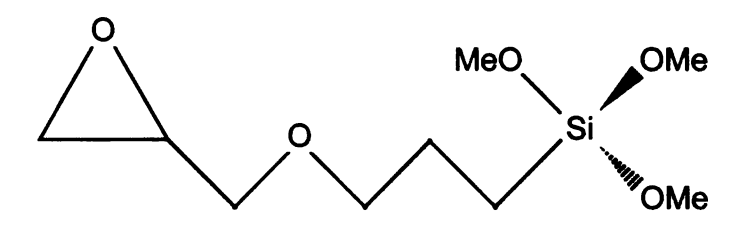


Figure 22: (3-glycidoxypropyl)trimethoxysilane[94]

In the silane treatment, the trimethoxysilyl part reacts with water to form a silanetriol which then bonds with the hydroxyl groups on the fibers (see Figure 23).

Figure 23: Silanization reaction. [94]

The organofunctional groups can react with the matrix.

#### 3.9 Fiber Selection

In the second phase of this research, larger composites were cured using glass fibers as well as treated and untreated natural fibers. Kenaf and hemp were selected for the fiber treatments (see Table 7). On Table 7, green indicates good properties, yellow indicates neutral properties, and red indicates poor properties.

Table 7: Fiber down selection table.

	Curing Curve/ Similar to Neat Epoxy	Degredation Temperature (°C) (5%)	ESEM	Loss Factor (ε")	% Mass Gain at Saturation
Kenaf	yes	64	better adhesion	0.04	16
Hemp	yes	105		0.07	16
Flax	yes	88	L	0.06	16
Henequen	yes	61		0.05	30

Hemp was selected because it had higher degradation temperatures than other natural fibers. Henequen was ruled out due to high moisture absorption. And Kenaf was selected over flax because it showed better compatibility with the matrix material in ESEM images. Hemp and kenaf fibers were then treated with alkali and silane.

#### 3.10 Microwave Curing Modes

Large samples were processed in a Lambda Technologies Vari-wave Model 1000 (see section 3.1 for more details on the apparatus). The composites were cured in a silicone rubber mold and capped with a Teflon lid. An infrared temperature probe was inserted at two points in the mold.

Two modes were used to cure the samples used for flexural testing. Each mode represents a specific electric field pattern within the microwave cavity. The modes were selected because they have minimal reflected power and can increase the temperature of the sample rapidly to decrease heating time. The locations of the temperature probes, T2 and T4, are shown in Figure 24. The curing program is designed to switch between two frequencies, one that primarily heats the center (T2) and one that primarily heats the edge (T4). When the temperature at T2 drops 3°C below T4 the frequency will switch to the one designed to heat T2 and vice versa. The goal is uniform curing of all the composites in the mold.

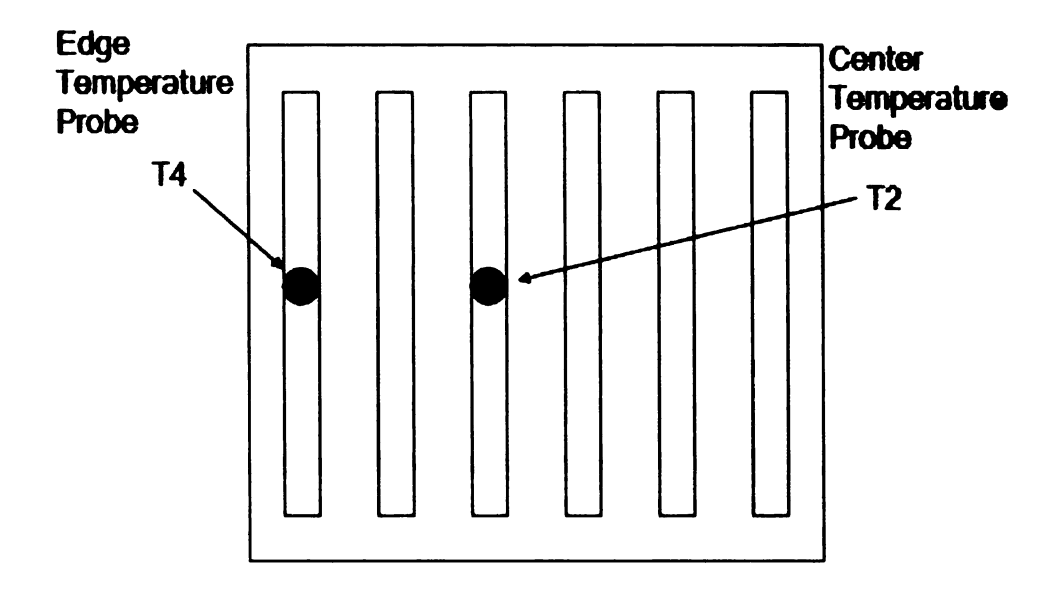


Figure 24: Schematic of mold for flexural testing showing the location of the temperature probes.

To find the frequencies which will provide even heating across the mold, the electric field strength was calculated at T2 and T4 using the following rectangular cavity equations [95].

$$A_z \neq 0$$
 for  $TM_z$  modes

$$\overline{E} = \frac{-j\omega}{k^2} \begin{bmatrix} k^2 + \partial x^2 & \partial xy & \partial xz \\ \partial yx & k^2 + \partial y^2 & \partial yz \\ \partial zx & \partial zy & k^2 + \partial z^2 \end{bmatrix} \begin{bmatrix} A_x \\ A_y \\ A_z \end{bmatrix}$$
(3.1)

$$A_z = \sin(k_x x)\sin(k_y y)\cos(k_x x)$$

$$E_z = (k^2 + \partial_z)A_z = 0$$

$$k^2 = k_x^2 + k_y^2 + k_z^2$$

$$k_x = \frac{m\pi}{a}$$

$$k_y = \frac{n\pi}{b}$$

$$k_z = \frac{p\pi}{c}$$
(3.2)

where  $\overline{E}$  is the electric field vector, k is the wavenumber, and A is the vector potential. The mode indices are m, n and p. The dimensions of the rectangular cavity are a, b and c, where  $a \ge b$ . Once a specific electric field is calculated that is high at T2 and low at T4 (or vice versa), its mode indices are then used to determine the resonant frequency [95].

$$f = \frac{1}{2\sqrt{\varepsilon\mu}} \sqrt{\left(\frac{m}{a}\right)^2 + \left(\frac{n}{b}\right)^2 + \left(\frac{p}{c}\right)^2}$$
 (3.3)

The chosen mode for position T2 was  $TM_{442}$  with a frequency of 3.4819 GHz and the chosen mode for position T4 was  $TM_{434}$  with a frequency of 3.5481 GHz. With these chosen frequencies the temperature difference between positions T2 and T4 did not exceed 3°C during the curing process.

### 3.11 Composite preparation for mechanical property testing

Fibers and epoxy were prepared as described earlier. The composite material was placed into the silicon mold and compressed using 156 psi of force in a Caver Press for 5 minutes. This was the greatest pressure that could be applied without severely deforming the mold. More material was then added to the silicon mold and it was compressed again with the same pressure at 100 °C for 15 minutes in the Carver Press. Pressure could not be applied during microwave curing due to processing constraints; materials used to mold or apply pressure must be microwave transparent. No pressure was applied during oven curing for comparison. Samples were then degassed in a vacuum oven for 20 minutes at 100 °C. Composites were cured in the microwave cavity and the conventional oven for 120 minutes.

### 3.12 Flexural Testing

Composites were prepared using treated and untreated kenaf and hemp fibers, glass fibers and a DGEBA/DDS matrix. A support span to depth ratio of 16:1 was used in accordance with the ASTM D 790-03 standard (see section A.9). The composite is bent until it breaks or 5% strain is reached. The crosshead speed used was 0.5 in/min, the span was 2.1 in and the loadcell used was 1000 lb (see Figure 25). Flexural modulus was determined with these experiments.

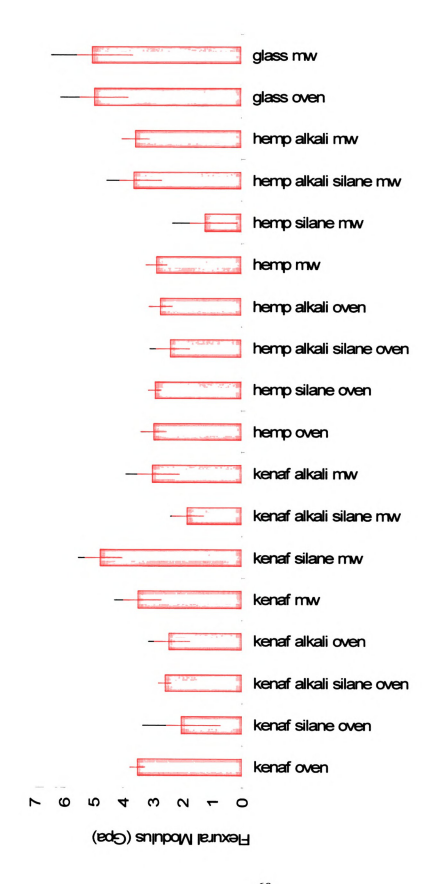


Figure 25: Flexural Modulus for treated and untreated composites.

Figure 25 shows the flexural modulus for the treated and untreated fiber reinforced composites. Glass fiber reinforced composites cured in both the microwave and oven and silane treated kenaf fiber reinforced composites had the highest flexural modulus. Silane treated hemp fiber composites had the lowest flexural modulus. Kenaf performed better in mechanical testing than hemp. Variation in mechanical properties is one of the major drawbacks to using natural fibers for composite reinforcement. The properties of natural fibers depend on the source, nature, and storage of fibers. This in turn affects the mechanical properties of the composites. The hemp used in this study was grown in Canada and the kenaf was grown in the United States. The age of the plant, the fiber's location on the plant, and the method used to extract the fiber from the plant can also affect the fiber properties [96]. Kenaf and hemp have significantly different cellulose and lignin content. Kenaf has 31 -39% cellulose and 15 - 19% lignin while hemp has 70.2 - 74.4% cellulose and 3.7 - 5.7 % lignin [1]. Cellulose forms the main structural component of the natural fiber's cell walls. Lignin is a cementing agent that holds fiber ultimates together in bundles. The kenaf stalk also contains a greater percentage of bast fibers (40%) than the hemp stalk (25%) [97]. The single fiber tensile strength of kenaf is 11.9 GPa while hemp is 9.0 [96]. This suggests that kenaf may be better for fiber reinforcement.

These results reinforce that variation in mechanical properties is one of the major drawbacks to using natural fibers for composite reinforcement.

## 3.13 IR Analysis of Kenaf and Hemp Composites

The infrared spectrum for untreated hemp and kenaf is shown in Figure 26. This analysis was performed to explain why kenaf performed better in the flexural testing than hemp.

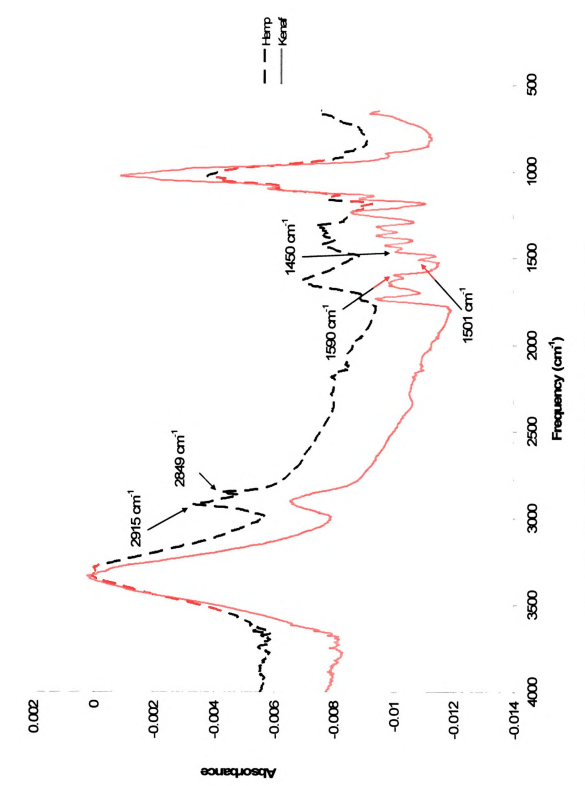


Figure 26: ATR - FTIR Spectra of hemp and kenaf (untreated)

Several peaks are present in kenaf that are not present in hemp.

The peak at 1590 cm<sup>-1</sup> represents an aromatic bond present in lignin [98].

Figure 27: Lignin monomeric unit.

The peak at 1501 cm $^{-1}$  is an aromatic C-H bond also found in lignin [99, 100]. The peak present at 1450 cm $^{-1}$  represents an asymmetrical CH $_2$  deformation of cellulose [98].

Figure 28: Cellulose monomeric unit.

In addition, a peak present in hemp is not present in kenaf. At 2849 cm<sup>-1</sup> is an OCH<sub>2</sub> symmetric stretching bond present in waxes [98]. The peak present at 2915 cm<sup>-1</sup>, C-H vibration in lignin and waxes, has a greater relative intensity in hemp than kenaf. These peaks indicate that hemp has more wax on the fiber surface than kenaf. Also that kenaf has more surface cellulose and lignin than hemp. The removal of wax increases adhesion between fibers and matrix materials [34, 85].

Increasing lignin and cellulose, indicated by the IR analysis, on the kenaf fiber surfaces provides more hydroxyl groups that can react with the epoxide groups in the epoxy resin. This may account for hemp's poor performance in mechanical testing and kenaf's relatively good performance.

### **CHAPTER 4: Kinetic Modeling**

#### 4.1 Introduction

The following sections cover the background of kinetic modeling of epoxies and the results of kinetic modeling on DGEBA/DDS reinforced composites.

# 4.2 Background

Epoxy groups react with amine via a ring-opening mechanism. The reaction is shown in Figure 29 [101]. In step 1, an epoxy group reacts with a primary amine to form a secondary amine. In step 2, another epoxy group reacts with the secondary amine to form a tertiary amine. In step 3, etherification, a formed hydroxyl group and an epoxy group react to form an ether crosslinking epoxy. Etherification is insignificant for stoichiometric mixtures.

Figure 29: Epoxy curing mechanism.

The hydroxide groups which are formed during the reaction can act as catalysts so that the reaction is autocatalytic, which is shown in Figure 30 [102]. The electron pair of the amine group bonds to the chain terminating carbon in the epoxy group, causing a bond breakage of the carbon-oxygen bond. The hydrogen atom detaches itself from the amine group and attaches to the oxygen

atom to form a hydroxide. The hydroxide group catalyzes further epoxy/amine addition by providing a hydrogen bond to the epoxy group.

### Uncatalyzed

$$R_1-NH_2$$
 +  $R_2$   $R_2$   $R_1$ 

### Autocatalyzed

Figure 30: Uncatalyzed and autocatalyzed epoxy curing reaction mechanisms

There are two types of kinetic models for the curing process [103]. One, mechanistic, is based on the reaction mechanisms while the other, phenomenological, is empirical. Mechanistic models offer better prediction and do not require curing experiments for each new

variable in the cure system. Phenomenological models offer more simple expressions with fewer kinetic parameters. Mechanistic models can often be difficult or impossible to derive due to the complex nature of the cure reaction. Therefore, phenomenological models have been used in most studies of epoxy cure kinetics. Following is a summary of phenomenological models for cure reactions and a summary of the DGEBA/DDS curing reactions.

The simplest phenomenological model is the n<sup>th</sup> order reaction kinetic model [104, 105], which expresses the kinetics as:

$$\frac{d\alpha}{dt} = k(T)f(\alpha) \tag{4.1}$$

where  $\alpha$  is the extent of cure, t is the time, the function  $f(\alpha)$  is expressed as  $(1-\alpha)^n$ , and k(T) is the overall reaction rate constant which obeys the Arrhenius relation:

$$k(T) = A \exp(-\frac{E}{RT})$$
 (4.2)

The  $n^{th}$  order reaction kinetics are simple to evaluate. According to this model, the maximum reaction rate should occur at the beginning of the reaction. However, in real cases,  $\alpha$ =0.3 - 0.4 at maximum reaction rate, which is better explained by the

autocatalyzed reaction mechanism [106, 107]. The reactions between amines and epoxy are autocatalyzed by the hydroxide groups formed in the reactions. The initial cure rate should be slow due to lack of catalytic hydroxide groups. The kinetic expression of autocatalyzed reaction for a stoichiometric reactant mixture is given by:

$$\frac{d\alpha}{dt} = (k_1 + k_2 \alpha^m)(1 - \alpha)^n \tag{4.3}$$

where  $k_1$  is the non-catalytic polymerization reaction rate constant,  $k_2$  is the autocatalytic polymerization reaction rate constant, m is the autocatalyzed polymerization reaction order, and n is the non-catalyzed polymerization reaction order. This model has been used to represent the cure kinetics of epoxy and unsaturated polyester cure systems [106, 108].

Thermal cure kinetic models have been used in modeling the reaction kinetics of microwave cured epoxy resins [71, 109]. It was demonstrated that the microwave cure kinetics of epoxy resin systems could be described by the autocatalytic kinetic model up to vitrification [71]. In the study of continuous-power and pulsed-power microwave curing of epoxy resins [109], a semi-empirical kinetic model was used:

$$\frac{d\alpha}{dt} = (k_1 + k_2 \alpha^m)(\alpha_u - \alpha)^n \tag{4.4}$$

where  $\alpha$  is the extent of cure,  $k_1$  and  $k_2$  are rate constants, m and n are constants, and  $\alpha_u$  is the ultimate extent of cure. This model is similar to the preceding model except that the ultimate extent of cure  $\alpha$  is included in the equation. This is due to the ultimate extent of cure is less than 100% due to gellation. This model was selected for this research.

### 4.3 Kinetic Modeling Results

Curing experiments were performed on neat DGEBA/DDS and hemp, kenaf, flax, henequen, and glass fiber composites at 145°C for both microwave and conventional curing methods. Differential scanning calorimetry was used to determine the extent of cure as a function of time. The average extent of cure was used in data regression to determine the kinetic parameters. The extent of cure vs. time data for microwave and conventional curing was obtained in the DSC experiments. See section A.1 for the procedure. In the regression, the data was fit to a 3<sup>rd</sup> order polynomial equation. The derivative of this equation was evaluated as a function of time. Kinetic parameters were then assigned initial values and the least square method was used to minimize the difference between the experimental data and the calculated data by solving for the kinetic

parameters. The experimental and calculated values are shown in Figures 31 - 42.

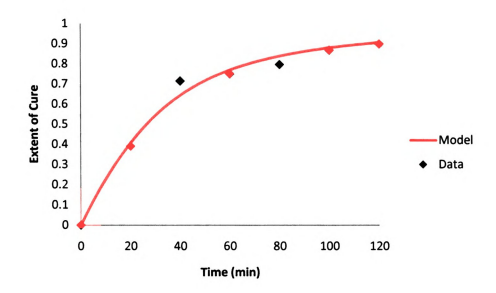


Figure 31: Curing curve for microwave cured hemp fiber composites.

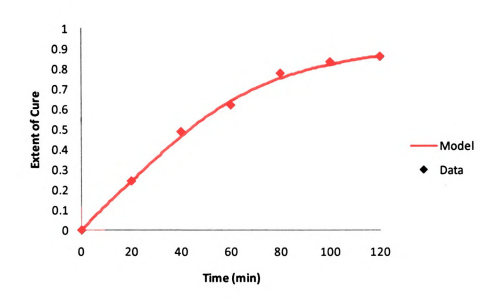


Figure 32: Curing curve for oven cured hemp fiber composites.

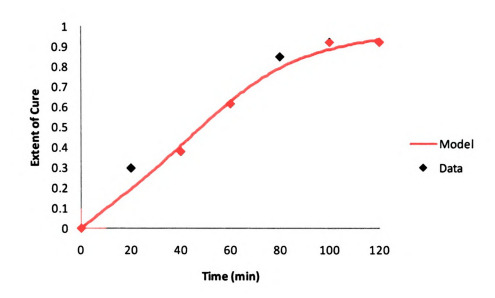


Figure 33: Curing curve for microwave cured kenaf fiber composites.

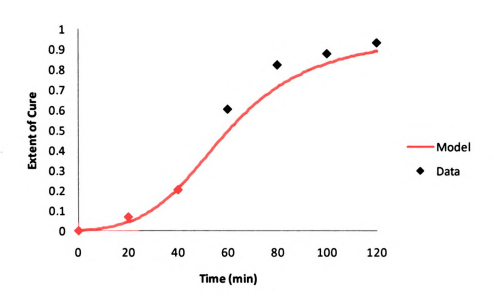


Figure 34: Curing curve for oven cured kenaf fiber composites.

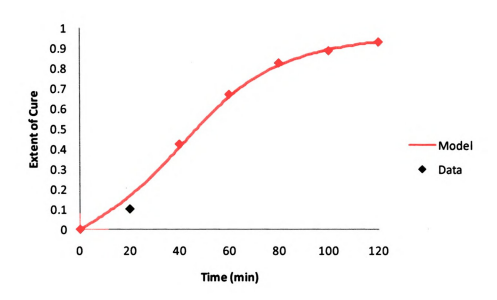


Figure 35: Curing curve for microwave cured glass fiber composites.

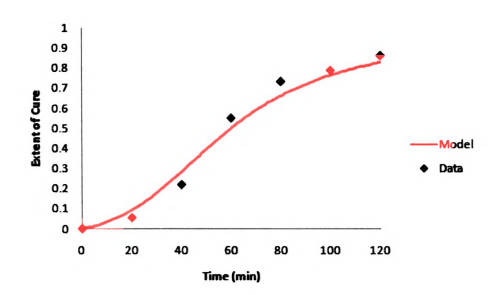


Figure 36: Curing curve for oven cured glass fiber composites.

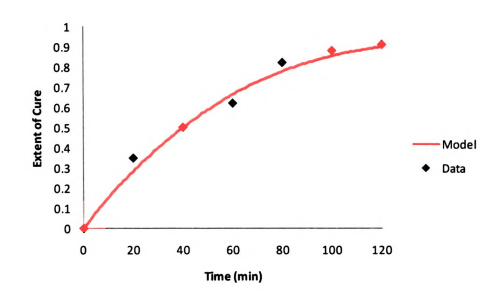


Figure 37: Curing curve for microwave cured flax fiber composites.

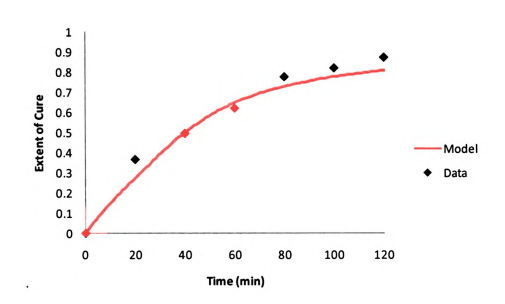


Figure 38: Curing curve for oven cured flax fiber composites.

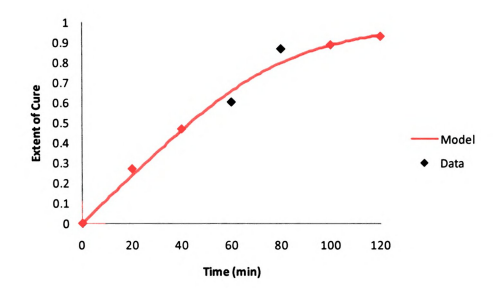


Figure 39: Curing curve for microwave cured henequen fiber composites.

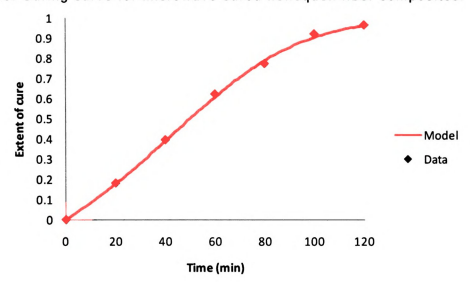


Figure 40: Curing curve for oven cured henequen fiber composites.

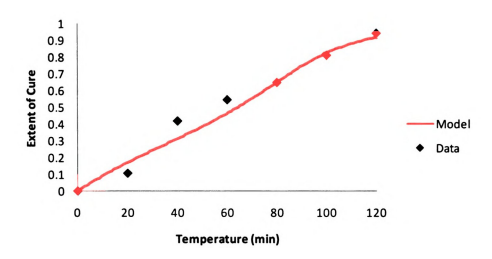


Figure 41: Curing curve for microwave cured neat epoxy.

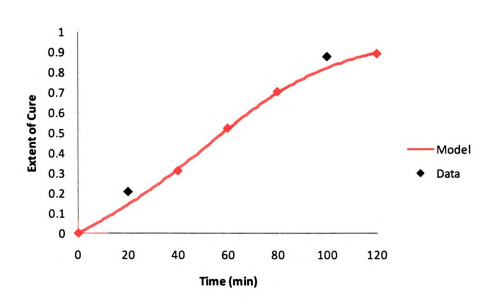


Figure 42: Curing curve for oven cured neat epoxy.

It can be seen from the figures that the curing curves have the typical shape of an autocatalytic reaction. The reactions between amines and epoxide are autocatalyzed by the hydroxide group formed in the reactions. Lack of catalytic hydroxide groups slows the

initial reaction. As the reaction proceeds and the maximum curing rate occurred at the extent of cure of around 0.3 to 0.4.

The values for the reaction order constants and the kinetic rate constants are shown in Table 8.

Table 8: Summary of kinetic constants for neat epoxy and natural and glass fiber composites.

	neat	neat epoxy	hemp	hemp	kenaf	kenaf	flax	flax	heneduen	heneduen	glass	glass
	epoxy mw	oven	MM	oven	MM	oven	MW.	oven	mw	oven	MM	oven
<u>₹</u>	0.010	0.007	0.027	0.014	0.010	0.004	0.020	0.019	0.013	0.008	0.007	0.003
<b>%</b>	0.23	0.04	0.05	0.10	0.07	0.14	1.98	0.43	0.03	0.03	0.09	90.0
Ε	3.68	1.36	1.58	1.90	1.89	1.38	3.53	2.55	1.63	1.28	1.54	0.95
۵	1.67	1.19	1.79	2.00	1.40	1.70	4.13	3.26	1.13	0.89	1.55	1.70

The autocatalytic rate constant  $k_2$  is greater than non-catalytic rate constant  $k_1$  for both microwave and thermal composites and for neat epoxy. This shows that the epoxy curing reaction is mainly an autocatalytic reaction. The non-catalytic rate constant is larger for microwave curing than for oven curing. This indicates that microwaves increase the activity of epoxide and amine groups, accelerating the non-catalytic reaction. The rate constant  $k_1$  is larger for microwave and thermally cured natural fiber composites than for glass fiber composites. The hydroxide groups present in the natural fibers may be responsible for this increase in the non-catalytic reaction. Kinetic constants in this work are similar to previous work except for the constant m [79] [80].

### **CHAPTER 5: Discussion of Results**

There is considerable interest in the field of natural fiber epoxy composites in structural applications, but no research has been done on microwave curing of these composites. The objective of these experiments was to develop high quality natural fiber epoxy composites, as a replacement for glass fiber composites, with reduced processing times using microwaves.

Natural fiber reinforced composites were proposed as an environmentally friendly replacement for glass fiber reinforced epoxy composites. Microwave processing was used as an alternative to conventional processing for these composites. To this end, cure time and extent of cure, thermal degradation, fiber and composite morphologies, and electrical properties were determined and compared with conventional thermal processing. Experiments were conducted to characterize the surfaces of treated and untreated fibers and to investigate the absorption of water in natural fiber composites. XPS and FTIR were used to determine the chemical composition of the fiber surfaces. ESEM images were taken to show the effect of the silane. Water absorption tests were used to determine the maximum water absorption mass of the natural fiber composites. Flexural tests were performed to determine the flexural modulus of the composites for comparison with glass fiber composites.

Natural and glass fiber composites have the same, relatively low, dielectric loss. Therefore the natural and glass fibers should interact in the same way with the microwaves. This was indicated by the curing studies in which the natural and glass fiber composites have similar curing curves. As curing begins, the epoxy is primarily heated by microwaves. At the end of curing, the fibers are primarily heated because the dielectric loss factor of the epoxy decreases as the curing progresses. Natural fibers and their composites have lower degradation temperatures than glass fibers and glass fiber composites. This affected the type of epoxy and the curing future natural fiber composites. temperature for thermogravimetric analysis also indicated that the natural fibers composites lost less than 5 wt% at 145°C so the curing temperature was not changed. The ESEM images show that epoxy clung to the surface of kenaf fibers pulled out of the composite fracture surface indicating that the bond between the matrix and fibers was strong. Epoxy did not adhere to the other fibers in the same manner. Alkali treated fiber composites absorbed more water than silane treated or untreated composites. This showed that the alkali treatment would not be a good choice for future natural fiber surface treatments because moisture absorption is already a challenge for natural fiber composites.

The TGA, water absorption and ESEM experiments were used to select which fibers would be selected for further testing. In the

second phase, larger composites were cured using glass fibers as well as treated and untreated natural fibers. Kenaf and hemp were selected for the fiber treatments. Hemp fibers were selected because it had higher degradation temperatures than other natural fibers at 5% weight loss. Henequen fibers were ruled out due to high moisture absorption. Kenaf fibers were selected over flax because they showed better compatibility with the matrix material in ESEM images. Modeling results show that the epoxy curing reaction is mostly autocatalytic.

FTIR experiments were conducted to examine the bonds present. Changes in the peaks in the FTIR spectrum at 1730, 1625 and 1239 cm<sup>-1</sup> showed that the alkali treatment partially removes hemicellulose and lignin from natural fiber surfaces, as indicated by the ESEM images. Electron microscopy also indicates the silane treatment increased the adhesion between the kenaf and the epoxy. XPS provided additional information on the composition of natural fiber surfaces, showing that the fiber surfaces have a larger proportion of lignin and waxes (than cellulose). Flexural modulus experiments were performed to test the effectiveness of the surface treatments. Silane-treated microwave-cured kenaf composites showed an improvement in modulus of 27% bringing it up to a similar modulus to glass fiber composites.

Kenaf and hemp fibers can replace glass fibers in reinforced epoxy composites provided lower processing and usage temperature

(less than 200°C), greater moisture absorption (4X greater than glass), and variability in mechanical properties is acceptable. Potential applications include automobile body parts [4, 26, 110], structural materials [111], and particleboard [90]. They have acceptable specific strengths and performed better in water absorption tests than henequen. Kenaf showed an increase in flexural modulus with silane treatment. Their low degradation temperatures restrict their processing conditions and restrict the choice of matrix materials to those with low curing temperatures.

Table 9: Summary of hemp, kenaf, and glass properties.

	F			5%		Flexural
	Curing Time (min)	Diele	ctric Loss Dielectric Constant (£") (£")	Degredation Temperature	% Mass Gain at 62 Days	(GPa)
d E	120	1.86926 ± 0.000	1.24834	104.63	16.8	$2.9 \pm 0.35$
<b>Senat</b>	120	$0.14102 \pm 0.03$	1.93949	64.27	16.3	$3.5 \pm 0.78$
Slass	215	$0.0501 \pm 0.014$	$4.7919 \pm .0004$	586.44	4.6	$5.04 \pm 1.38$

Microwave curing shows promise as a processing method for natural fiber composites. There are advantages in curing time and energy consumed. However, more work needs to be done to design a microwave cavity that can cure larger composites and apply pressure to the composites during the curing process before microwave processing can produce better quality samples.

# **CHAPTER 6: Energy and Economics**

Ultimately kenaf proved to be the better reinforcement material compared to hemp, henequen, and flax. Kenaf performed better in mechanical testing than hemp, and henequen and flax were ruled out prior to mechanical testing (see Section 3.9 for the discussion). Kenaf and glass composites will be further compared in this chapter.

There are many steps involved in making kenaf fibers available for use in natural fiber composites including growing, harvesting, drying, retting, bailing, and processing (see Figure 43).

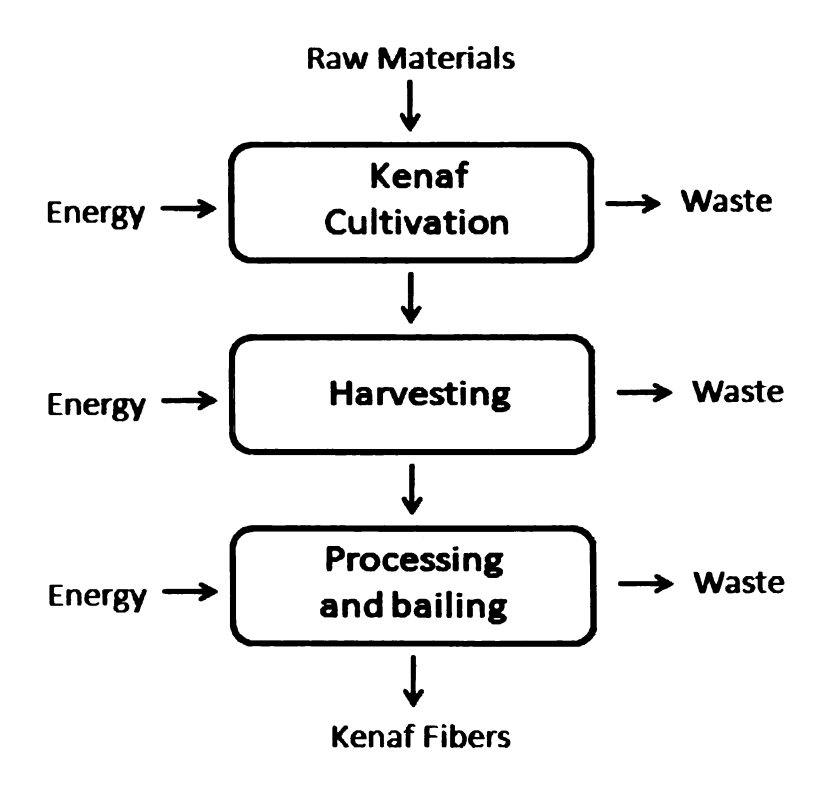


Figure 43: Process flowchart for kenaf fiber production.

Kenaf plants are grown annually from seeds. Plants can be harvested by hand using a sickle or mechanically with special harvesters that utilize high-tensile steel [2, 92]. The plants can then take up to 14 days to dry [92]. The retting process removes pectin and lignin from the stalk to separate the bark from the core and the fibers are separated from the bark fabric [2, 92]. Retting can be performed by immersing the fibers in water, using dew or rain, mechanically, and chemically using sodium hydroxide [2, 92]. The fibers are then dried again and formed into round or rectangular bales [92]. Processing consists of several steps: opening the bales, elimination of impurities, metering the stalks, decortication of the fibers, and cleaning and separation [92]. The bales can be opened with three types of machines: guillotine, hopper feeder, and bale cutter. These machines not only open the bales but they also cut the fibers into sections. The hopper feeder can only handle rectangular bales while the other two can handle both types [92]. Pieces of metal and stones are detected and removed in the next step. The metering processing step transforms the stalk bunches from the bale into a continuous stream of stalks. Decortication separates the fibers from the wood using one of three methods: breaking rollers and swing-hammer mills with and without cleaning [92]. The cleaning step removes small pieces of wood (shives) and dust from the fibers. This cleaning process is done mechanically [92]. The short fibers are then separated from the long fibers. The production of 1 kg of kenaf fibers requires 0.089 MJ of electricity [112]. Worldwide kenaf production is  $9.7x10^5$  tonnes per year [110] at a cost of \$60.5 per tonne [113].

Glass manufacturing requires four steps: batch preparation, melting and refining, forming, and post-forming (see Figure 44) [114].

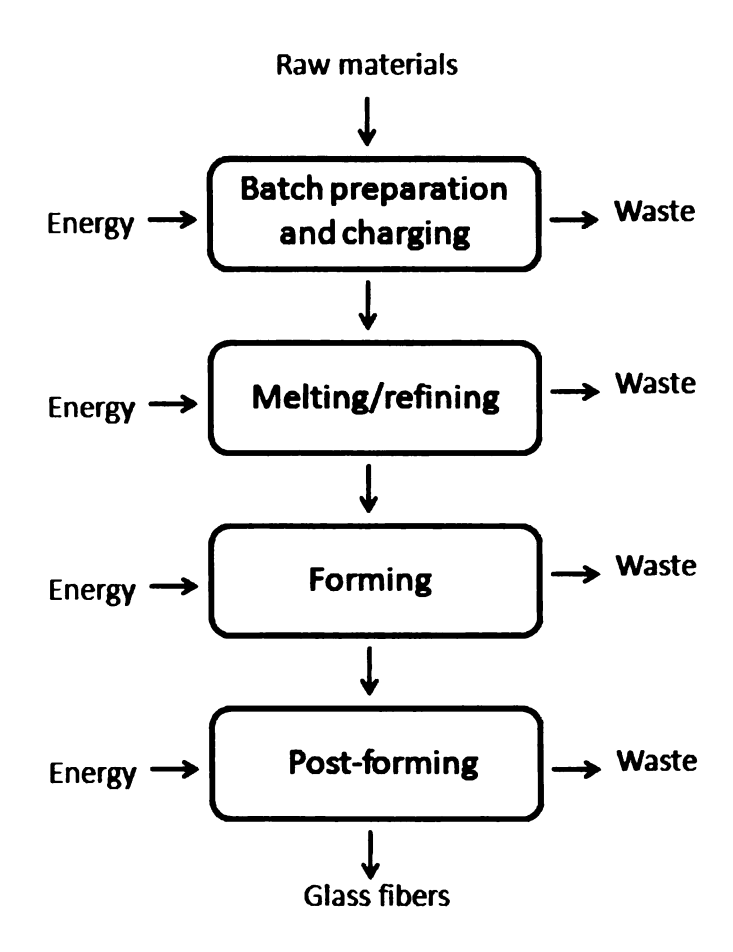


Figure 44: Process flowchart for glass fiber production.

During the batch preparation step, materials such as formers, fluxes, stabilizers, and colorants are mixed to prepare them for the melting process. Proper mixing is required to avoid a mixture that is

not homogeneous. This can result in a melting time increase, viscosity differences, and inferior product quality. This mixture is then moved to a furnace. In the furnace, the batch experiences melting, refining, homogenizing, and heat conditioning [114]. Refining removes gas bubbles from the glass. Mixing, time, and temperature are some of the factors that can affect the homogeneity of the molten glass. Thermal conditioning brings all the glass material to the same temperature. Glass fibers can be made after the molten glass cools to a suitable temperature or the glass can be formed into marbles for melting again later [114]. E-glass fibers are formed by pushing the melt through small holes. The resulting fibers are coated with coupling agents or sizings and wound onto a spindle. These fibers are finished in an oven to dry the coupling agents or sizings. Then the sizings or coupling agents are cured, also in an oven. Fibers may then be chopped, twisted, woven, and finally packaged [114]. The total (electricity and fuel) energy required to produce 1 kg of glass fibers is 9.71 MJ [112]. Over one million tons of glass fibers are produced in the US per year [114]. Glass fibers cost \$3.25 per kilogram [1].

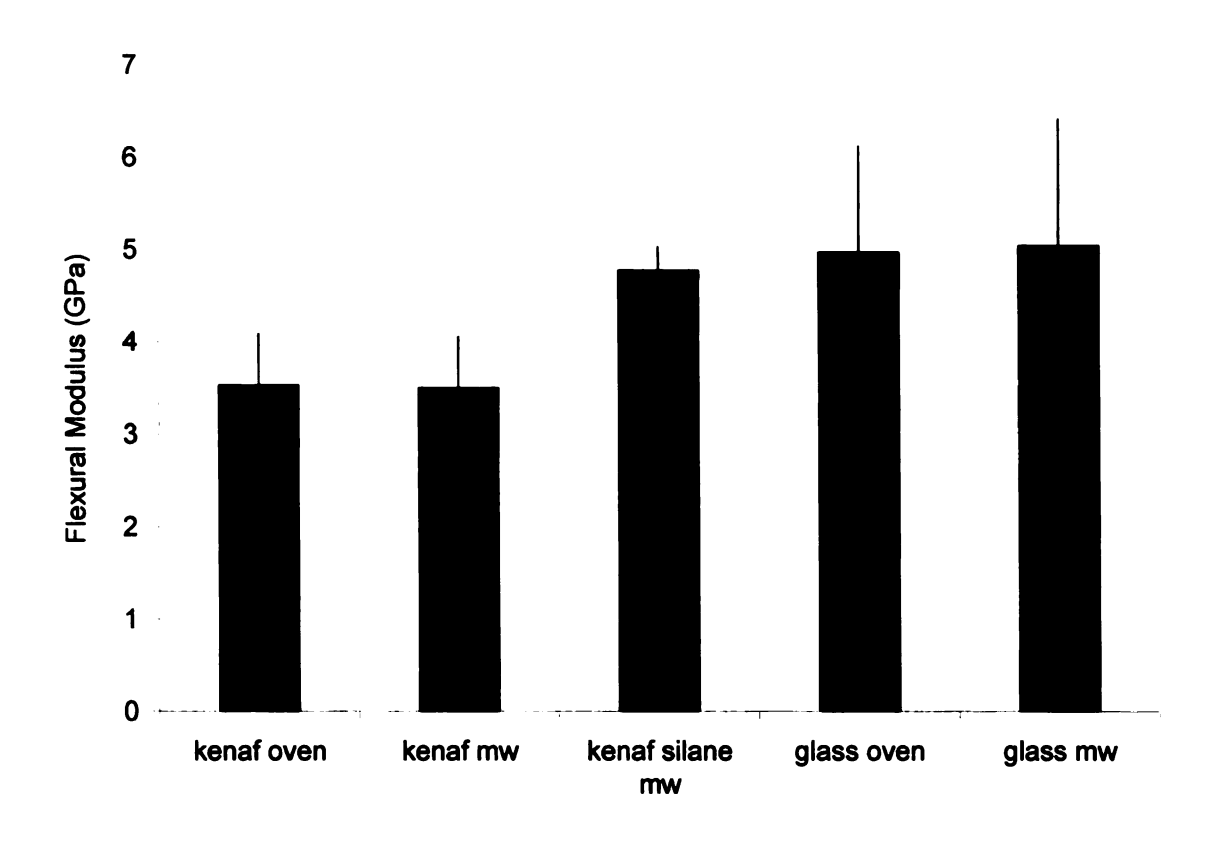


Figure 45: Flexural modulus comparison for kenaf.

Oven cured and microwave cured kenaf composites have similar flexural modulus, showing both cure methods are equally viable curing methods (Figure 46). However microwave processing is superior due to the energy savings compared to conventional ovens. Composites require 60 - 65 W to cure in the microwave where oven cured composites require 1600 W. However, up to 12 sets of samples can potentially be cured simultaneously in the oven so the more conservative estimate is 432 KJ for microwave cure vs. 936 kW-h for oven curing (for one set of composites). This is still a considerable energy savings. With microwave processing, the

composites reach the cure temperature in approximately 20 minutes.

Oven processing required approximately 95 minutes.

Silane treated kenaf shows an improvement in modulus (27%). This fundamental observation shows that the silane surface treatment improves adhesion between the kenaf fibers and the DGEBA/DDS matrix. This is also visible in the ESEM micrographs (see Figure 21). Results for different fiber reinforced composites examined in literature were dependant on the fiber and matrix material used (see section 2.1). The fiber/matrix combination researched in this work had not been previously studied.

Natural fibers have reduced production costs and greater energy savings than glass.

Table 10: Energy and economics for kenaf and glass.\*

	Fuel (MJ/kg)	Electricity (MJ/kg)	Total Energy Fuel + Electricity (MJ/kg)	Total Cost of Fuel (\$/kg)	of	Total Cost Fuel + Electricity (\$/kg)
Glass	48.13	9.71	57.84	1.63	0.201	1.83
Kenaf	0.96	0.089	1.049	0.03	0.002	0.03

<sup>\*</sup> The fuel and electricity requirement were taken from a life cycle analysis of kenaf and glass fibers [112].

The economics calculations assume a diesel cost of \$4.35/gal and an electricity cost of \$0.0752/kW-h. There is a 98% saving in energy and cost by producing kenaf fibers instead of glass fibers

(see Table 10). There is a 95% savings in energy and energy cost by switching from 30 vol% glass fibers to 30 vol% kenaf fibers in a polypropylene composite (see Table 11).

Table 11: Economics for kenaf and glass composites.

	30 vol % glass		30 vol % kenaf		45 vol % kenaf	
	volume of glass (m <sup>3</sup> )	volume of PP (m³)	volume of kenaf (m³)	volume of PP (m³)	volume of kenaf (m³)	volume of PP (m <sup>3</sup> )
	0.3	0.7	0.3	0.7	0.45	0.55
Energy Cost to Produce						
(\$/m3) Total Energy Cost to Produce	4.644	0.254	0.013	0.254	0.019	0.200
(\$/m3)	;	4.90	\$0	.27		\$0.22

Energy can also be saved with natural fiber composites by increasing the fiber content relative to glass fiber content. This reduction in the volume of matrix (polypropylene) used reduces energy consumption and energy costs for kenaf fiber reinforced composites by 18%.

Natural fiber composites can also benefit society by reducing pollution. For example, natural fiber composites are being incorporated into cars which can reduce the vehicle's weight, increase its efficiency and reduce gas emissions [83]. Natural fiber composites also cause less wear on process equipment which would have to be disposed in landfills. If natural fibers are combined with a

biopolymer matrix, the product can potentially be completely recycled.

Natural fiber production can benefit farmers as a complementary crop for cotton and soybeans (in the United States) [113]. Using natural fibers for composite reinforcement can reduce waste from fields if they are already being incorporated as complementary crops [41]. Natural fiber production may also provide employment and economic growth in rural areas [96]. Natural fibers such as hemp and flax can clean metals from the soil [115]. Sisal and henequen are drought resistant crops [115].

Using natural fiber composites may help meet government legislation requirements. In the European Union, the End of Life Vehicles Directive requires 85% of vehicles to be recycled by 2015. The End-of-Life Vehicle Recycling law in Japan requires 95% to be recycled by 2015. In the United States, the 2002 Farm Bill (Title IX) supports increased use of biobased products with programs and grants. It also requires federal agencies to purchase biobased products in certain categories.

Switching to natural fibers from glass fibers for composite reinforcement offers cost, time, and energy savings.

#### **CHAPTER 7: Conclusions**

In this study, research on microwave processing of natural fiber and glass fiber reinforced composites was conducted in two phases. The first phase focused on untreated natural fibers and glass fibers alone and on small composites with untreated natural fibers or glass fibers. The second phase focused on untreated, alkali treated, and silane treated natural fibers and on larger composites with treated and untreated fibers.

In the first phase, differential scanning calorimetry, dielectric testing, and thermogravimetric analysis were conducted on the untreated fibers and composites. Small samples of kenaf, flax, hemp, henequen, and glass composites were cured using microwave and oven curing. The resin used was diglycidyl ether of bisphenol-A with diaminodiphenyl sulfone used as a curing agent. Differential scanning calorimetry was performed to determine the extent of cure of the composites. Microwave cured composites faster than oven cured composites. Microwaves increase the activity of epoxide and amine groups which accelerates the non-catalytic reaction. Dielectric tests were performed to determine the dielectric properties of the fibers and the composites. Dielectric experiments showed that the uncured epoxy is preferentially heated, relative to the fibers, at the beginning of the curing cycle due to its relatively large loss factor. However, the loss factor of the epoxy decreases with cure, eventually dropping below the loss factor of the fibers. At this point the fibers will be preferentially heated. Dielectric experiments also showed that the natural fibers all have the same dielectric loss so they should cure at the same rate with microwaves. Thermogravimetric analysis was conducted to determine the degradation temperatures of the fibers and composites. Natural fiber composites had lower degradation temperatures than glass fiber composites. This was expected because natural fibers have much lower degradation temperatures than glass fibers (which did not degrade at the temperatures tested). All composites had less than 5% weight loss at the curing temperature.

In the second phase, alkali and silane treatments were applied to kenaf and hemp fibers. Hemp was selected because it had a higher degradation temperature than the other natural fibers. Henequen was ruled out due to higher water absorption. Kenaf was chosen over flax because it had better adhesion to the DGEBA/DDS matrix (seen in ESEM images). The fibers and composites were analyzed using Fourier transform infrared spectroscopy, X-Ray photoelectron spectroscopy, water absorption testing, environmental scanning electron microscopy, and flexural testing. The Fourier transform infrared spectroscopy provides the spectra of the surfaces of treated and untreated fibers. FTIR experiments show that the alkali treatment removes hemicellulose and lignin from fiber surfaces. X-ray photoelectron spectroscopy provides atomic

concentrations on the surfaces of treated and untreated fibers. XPS experiments show that fiber surfaces have greater proportions of lignin and waxes than of cellulose, hemicellulose, and pectin. Water absorption tests determine the mass of water absorbed into composite samples over time. The untreated henequen composites absorbed the most water while glass fiber composites absorbed the least. Alkali treated hemp and kenaf composites absorb more water than other treated fiber composites. Environmental scanning electron microscopy was used to observe fiber surfaces and composite fracture surfaces. ESEM experiments show interfibrillar material is removed by the alkali treatment. The experiments also show that the silane treatment is effective in increasing the adhesion between the fiber and matrix. Flexural testing was performed to determine the flexural modulus of the natural fiber and glass fiber composites. Glass fiber composites had a greater flexural modulus than untreated and treated most natural fiber composites with the exception of silane treated kenaf. The silane treated kenaf showed an increase in flexural modulus of 27%. Oven processing required approximately two times the energy to cure one set of composites as microwave processing.

Microwave processing of natural fiber composites has not been previously examined in literature. Epoxy composites reinforced with chopped kenaf, hemp, flax, or henequen fibers can be cured 75 minutes faster in the microwave than in the oven. The dielectric

properties of natural fibers were studied and compared to glass fibers. It was found that the dielectric loss factor of all the fibers were similar, so all the fiber composites examined should interact with microwaves in a similar manner. This was confirmed with the DSC experiments since all the DSC curves were similar.

Silane treated kenaf fiber reinforced DGEBA/DDS composites can replace glass fiber reinforced composites provided that the curing and use temperatures are kept relatively low (<145°C), that the composite is used in a low moisture environment, and consistent mechanical properties is not critical.

### **CHAPTER 8: Future Work**

This work focused on producing natural fiber composites produced by microwave processing as a replacement for glass fiber composites. Several problems arose during these experiments that have not yet been resolved. Applying pressure to the composites during the microwave curing process would improve the mechanical properties considerably. Some researchers have used a vacuum bag or autoclave system to apply pressure during curing [116-118]. Using a vacuum bag will reduce the void fraction and apply pressure to the composite. The pressure used is limited by the partial pressures of the components in the resin [117]. Resin will be removed if the pressure is too low. The viscosity of the resin system is also a limiting factor in the use of vacuum bagging. Resin will be removed from the composite if the viscosity is too low and voids will not be removed if the viscosity is too high [117]. Note that during the cure, the viscosity of the resin system will change. During the autoclave process, the applied pressure removes voids by dissolving them in the resin material. The pressure required for this dissolution to occur increases as the viscosity increases. The autoclave method can be used in conjunction with vacuum bagging [117].

The variability in mechanical properties introduced by the natural fibers should be also addressed. Chemical composition, fiber surface properties, strength, crystallinity, and stiffness can vary among fibers of the same type [119]. Some of the variability in fiber

properties can be mitigated by choosing fibers from the same source and of the same age. Dew retting is commonly used to extract natural fibers from their plants and this method introduces significant variation in fiber properties because it is dependent on the weather. Using glycophosphate or enzyme treatments during the retting process is being studied to make the fiber properties more consistent from season to season. When glycophosphates are added during dew retting the yield and quality were similar to water or dew retting without glycophosphates [92]. However, the addition of glycophosphates increases the time required for retting which would impact future crop cycles. The enzyme pectinase is necessary for retting to take place. Adding additional pectinases to water or dew retting processes increases the fiber yield and the fibers have comparable qualities to the untreated fibers [92]. The fibers require added processing to remove or denature the enzyme after retting is complete [92]. The impurities, such as wood-like core material, left over from the pre-processing to extract the fibers should be removed before composites are produced. These impurities can initiate cracks in the composites [120].

The effect of fiber inclusion fraction on composite curing and mechanical properties should also be studied. Arib *et al.* studied the effect of increasing pineapple leaf fiber volume fraction on the mechanical properties polypropylene composites [121]. Tensile modulus and strength were found to increase with increasing fiber

fraction up to 16.7% where it decreases. They attribute this decrease to higher void content, fibers acting like flaws instead of reinforcement at high fiber volume fraction, poor fiber alignment, and low interfacial shear strength. Luo *et al.* examined varying the fiber volume fraction of pineapple fiber reinforced PHBV composites [122]. They determined that tensile strength and modulus decrease in the transverse direction and increase in the longitudinal direction as the fiber content increases. They observed that increasing fiber volume fraction increases the void fraction. Increasing void content leads to decreasing mechanical properties. Shaikh *et al.* also found that increasing natural fiber volume fraction increased the strength of the composite [123].

Curing larger samples for testing with flexural testing revealed another problem: uneven curing with microwave processing. Developing a multiport microwave cavity, an alternative to variable frequency processing, will enable curing of larger composites. A multiport cavity utilizes mode switching, like the cavity used in this work. However, in a multiport cavity the mode switching is done by changing the power delivered to different ports as opposed to changing the frequency in a single-port system. Previously, work has been done on modeling a cylindrical multiport cavity [124]. The cavity had two feed ports; one excited a TE mode and one a TM mode. The ports were designed to minimize the power entering through one port and exiting through the other and maximize the

power entering the desired sample. Modeling the multiport cavity system requires a coupled electro-, thermo-, and kinetic model. This model would be used for improving process control and selecting matrix or reinforcing materials.

These future experiments will improve composite properties of microwave cured samples by increasing the pressure during cure, curing larger sample evenly, and by reducing the variability of natural fiber properties.

**APPENDICES** 

## Appendix A: Material Characterization Methods

## A.1 Differential Scanning Calorimetry (DSC)

Differential Scanning Calorimetry is used to study thermal transitions in polymers such as glass transition, crystallization and melting [125]. This method uses a sample pan and a reference pan heated at the same rate and records the difference in heat flow between the two pans. This is plotted against temperature to determine the thermal transitions (Figure A1).

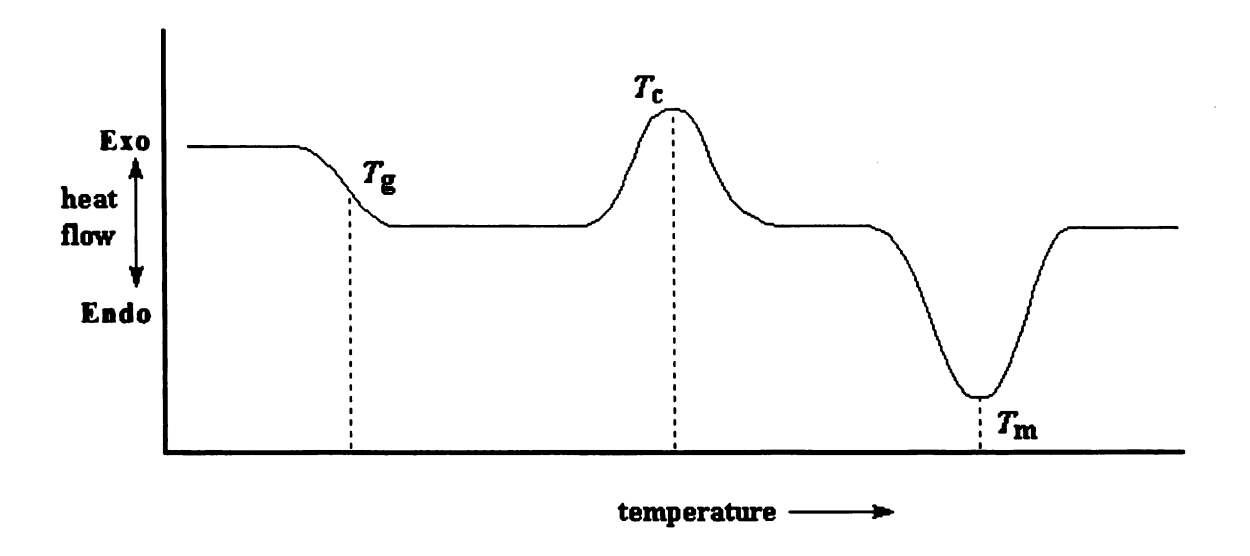


Figure A1: A sample DSC plot of thermal transitions.

The glass transition temperature is the first temperature shown in the above figure. This indicates a change in the polymers heat capacity and properties. Polymers are more brittle below their  $T_g$ . The crystallization ( $T_c$ ) and melting temperatures ( $T_m$ ) are shown next on the figure. These peaks appear for polymers with crystalline

regions. The heat of reaction, Q, is the area under the crystallization curve. The extent of reaction calculation,  $\alpha$ , for a sample cured 20 minutes is shown below.

$$\alpha = 1 - \frac{Q_{20}}{Q_{uncured}} \tag{A.1}$$

### **Procedure**

- Place 5 10 mg of the composite in a solid sample pan
- Crimp the pan closed
- Place the sample pan and the reference pan in the DSC sample chamber
- Ramp the temperature from room temperature to 180 °C at 5
   °C/min
- Cool the sample chamber back to room temperature and remove the samples
- Plot temperature vs. time
- Calculate α
- Plot α vs. time

### A.2 Dielectric Tests

The perturbation method will be used to determine the dielectric properties of the natural fibers and composites [80].

#### Procedure

- Set Start on the oscillator to 2.44 GHz and Stop to 2.46 GHz.

  Set the sweep time to 0.01.
- Turn the RF output on.
- Turn the Microwave switch to Auto (bottom position).
- Load the program in Labview (automated\_test5.vi)
- Follow the instructions in the program with regards to disconnecting the switch from the cavity.
- Lower the empty sample holder to the bottom of the cavity.
- Move the sample holder up until the oscilloscope shows the largest frequency shift (to the left). The sample will be centered.
- Center the null at 2.45 GHz by changing the cavity length.
   Record this cavity length.
- Adjust the probe depth to get the lowest SWR possible. Cavity length may need to be readjusted.
- Click Save Data to get the frequencies that cross SWR = 2
   (DFc). Enter the filename.
- Remove the sample holder form the cavity, prepare the sample.
- Load the sample into the holder, and lower the sample holder to the bottom of the cavity.

- Re-center (use CF) the sample and adjust the probe depth if necessary. Do not adjust the cavity length.
- Push Save Data to record the new null frequency (Fs) and the frequencies that cross SWR = 2 (DFs).
- Turn the RF power output off.
- The resonant frequency shift (SFs) is (Fc Fs) x 1000.
- Remove the sample from the cavity.
- Use the program Microwave Processing and Dielectric
   Diagnostic System (Windows Explorer/diane) to calculate the dielectric properties.
- Press spacebar then 3 for "Swept Frequency Dielectric
   Measurement Program". Press 2 for "Absolute dielectric
   measurement for liquid/powder materials."
- Input the radius of the cavity (Rc), the radius of the sample holder (Rs), the sample weight, and the sample density. Press Enter several times to move the cursor to the next row.
- Input the cavity length, the initial frequency (Fc) and the initial half-power bandwidth (DFc). Press Enter several times to move the cursor to the next row.
- Input the new resonant frequency (Fs), the new half-power bandwidth (DFs) and the resonant frequency shift (SFs). Press enter several times until the dielectric constant and loss factor appear.

- Press Enter a few more times to save the results. Enter a file
   name and press Enter again.
- Press ESC to return to the previous menu.

## A.3 Thermogravimetric Analysis (TGA)

In thermogravimetric analysis, a sample is placed in an inert-gas temperature controlled environment [125]. The weight loss or gain is recorded as a function of time and temperature. The temperature can be increased linearly or held isothermal in the furnace. This method can determine the decomposition temperatures of the fiber reinforcement materials and matrix of the composites. A TA Instruments Hi-Res TGA 2950 was used.

#### Procedure

- Check the gas levels.
- Fill out the sample information in the program.
- Put an empty DSC pan (bottom) into the basket.
- Push TARE on the machine.
- Put the sample in the pan (10 30 mg).
- Push LOAD on the machine.
- Wait for the sample weight to read a steady value (# means unstable).
- Push FURNACE on the machine

- Push START in the program or on the machine to run the program (when it says complete)
- Wait until the temperature is below 30 degrees before pushing
   TARE for the next sample.

#### A.4 Surface Treatments

Surface treatments are used to increase the adhesion between the natural fibers and the epoxy.

## Silane Procedure [36]

- Make 1% solution of silane Z-6040 with DI water & ethanol (1:1). Keep pH=4 with glacial acetic acid. Mix solution in plastic container.
- Close lid and use magnetic stirrer under hood for 2 hours.
- Soak fibers in solution for 1 hour.
- Dry fibers in hood for 12 hours.
- Dry fibers in oven at 100 °C for 5 hours.

# Alkali Procedure [33]

- Make solution of 5% NaOH in DI water using magnetic stirrer.
- Immerse fibers in NaOH solution for 1 hour.

- Make solution of tap water and glacial acetic acid (2%) (pH
   = 6).
- Wash fibers with tap water until all foam and alkali is gone.
- Neutralize fibers in acid solution for about 20 minutes.
- Wash fibers with DI water.
- Dry fibers for 24 hours in the hood.

# A.5 Fourier Transform Infrared Spectroscopy (FTIR)

Attenuated total reflectance FTIR was used to obtain the spectra of the treated and untreated natural fibers. These spectra can be used to identify functional groups on the fiber surface. A Perkin Elmer Instruments Spectrum One with the Attenuated Total Reflectance (ATR) technique was used [126].

### Procedure

- Select 'Background' (only done for the first sample)
- Check the top plate, click 'OK'
- Change the directory to your own
  - Select 'Setup', 'Options', and the 'File' tab
- Select 'Monitor' from the toolbar at the top
- Select 'Monitor Sample'
- Select 'Absorbance'
- Select 'Toolbox' from the toolbar in the menu box

- Load the sample over the diamond and clamp it down. The arm should be as far to the left as it can go. Force should be around 40 (the maximum force you can use is 100). You may need to press 'Auto Y' at the side of the menu box to keep the entire spectrum on the display.
- Select 'Stop'
- Name the sample and click 'apply'
- Select the 'Scan' tab
- Change 'Units' to 'A' and select 'Apply' (Range Start: 4000,
   End: 650, Scan Type: Sample, Scan #: 4)
- Scan the sample again
- To adjust for penetration depth, select 'Process', 'ATR
   Correction' and set 'Contact' = 0. The new curve is the
   corrected data. Delete the old curve.
- Click 'Peaks' or 'Setup', 'Options', 'Peak', and set 'ABS' =
   0.001 to label the peaks. The peaks can also be labeled manually by selecting 'Cursor' and dragging the line to the desired peak then selecting 'Label'
- To change the samples, select 'Monitor' and take the sample off
- Clean the top plate with acetone well. Only rub the surface in one direction or you will reapply the contaminants

## A.6 X-ray Photoelectron Spectroscopy (XPS)

XPS will be used to investigate the elemental composition of the treated and untreated fiber surfaces [127]. The characteristic energies of secondary electrons released from the surface of the samples, bombarded with x-rays, are recorded and analyzed. XPS was performed by Per Askeland. An Electronics PHI 5400 ESCA system was used.

# A.7 Water Absorption

Water absorption tests are conducted due to the affects this absorption has on composite properties such as stiffness and strength. There are two types of absorption tests. Tests conducted for a set amount of time are called fixed conditioning. Those conducted until the sample reaches equilibrium with its environment are equilibrium conditioning. Surface area, temperature, fiber content, thickness, and relative humidity are all factors in the rate of moisture absorption into a composite. The absorption tests were conducted according to the guidelines in ASTM D5229 (for equilibrium conditioning).

#### Procedure

 The natural fibers flax, kenaf, hemp, and henequen were soaked for 1 hour in hot RO water around 80°C.

- The fibers were then allowed to dry on metal foil at room temperature for 48 hours.
- The fibers were further dried in an oven at 100°C for 4 hours and then placed in airtight plastic bags to keep out moisture.
- A stoichiometric amount of diglycidyl-ether-of-bisphenol-A(DER) epoxy resin and 3,3-diamino-diphenyl-Sulfone(DDS) curing agent were pre-weighted along with the amount fiber cut to ¼ inch lengths that would produce samples with 15wt% fiber content.
- In addition to the four natural fibers mentioned previously,
   glass fibers cut to ¼ inch strands were also used.
- After heating the DER to ease mixing, the DDS was added to the DER and mixed with a magnetic stirring bar until the solution became transparent with a yellow tint.
- The appropriate fibers were then added to the solution and mixed with a spatula until the fibers were uniformly wetted and coated with the epoxy resin solution.
- The mixture was then pressed by a spatula into a 4.0cm by
   2.7cm by 3.0mm mold coated with a mold release agent.
- The mold was then placed in an oven with metal blocks placed on top of the mold to provide compression.
- The samples were cured in the oven for 2 hours at 145°C.

- After curing, the samples were removed from the mold, and fine sandpaper was used to file away any rough faces of the samples.
- Altogether, 10 samples of each fiber composite were made.
- Preceding the water absorption test, all the samples were dried in an oven for 1 hour at 50°C to remove any excess moisture.
- The samples were then cooled to room temperature in a desiccator.
- After their dry masses were recorded, they were immersed in distilled water at room temperature.
- At appointed time intervals each sample was removed from the water and dried by paper towel until no more water readily left the sample.
- This was done to remove any water on the surface or pooled in voids, air pockets, or uncoated sections of fiber.
- The mass of the sample was recorded and then re-immersed in distilled water.
- The wet mass of the samples was recorded at 6, 24, 48, and
   72 hours and then once a week until a maximum mass was achieved.
- The recorded masses were then used to calculate the percent mass gained

# A.8 Environmental Scanning Electron Microscopy (ESEM)

ESEM will be used to observe the microstructure of the samples. Unlike conventional SEM, ESEM can be operated with relatively high pressures (up to 10 torr) in the sample chamber. Water is used as the imaging gas and its vapor pressure can be controlled with a vacuum pump. Electrons ejected from the sample, secondary electrons, collide with the water molecules and are detected by a gaseous secondary electron detector [128]. It is sometimes necessary to gold coat the samples to avoid charging. A Philips ElectroScan 2020 ESEM was used.

#### Procedure

### Startup:

- Check to make sure the pressure in the gun is less than 10<sup>-6</sup> torr (in the cabinet below the computers, on the right).
- Push the green button, Console On
- Hit 'Return' on the left keyboard when the computer asks for a password
- Set 'Beam kV' to 15 kV (right mouse button makes it go faster)
- Go to 'Gun' then make sure the 'setpoint' is at 1.83 A and the 'ramp time' is 1200 sec
- Click 'Heat Filament' in the 'Gun' menu.
- In 'Vacuum Control' click 'vent'

• Load the sample and click 'wet' after you shut the door

## Alignment:

- Click 'Ghost' then 'Gun'.
- Click 'Source', drop magnification down to 40X
- Turn the brightness down and the contrast up to see the beam
- Turn the condenser down to 40% (if there is streaking, turn down the contrast)
- Adjust the column (2 knobs) to the center of the scan mode box.
- Adjust the gun (3 knobs on the top of that apparatus) to get the beam in the center of the circle.
- Turn the condenser up to 43, 46, 50 and 53% repeating the adjustments each time.
- Reduce the condense down to 50%
- Turn 'Source' off.
- Adjust to at least 7000x and focus.
- Click 'Column'
- The x and y stigmation should be zero
- Click Wobble and adjust the column knobs until the movement is reduced
- Click Wobble and return

- Under 'Image Disk', select '1K', and then click 'burn'. This puts
  the info at the bottom of the picture. From left to right: voltage,
  magnification, focal length, pressure.
- Vacuum Control should be between 2.5 and 4.5 torr
- Scan time should be around 0.48 sec
- If there's sparking, turn down the contrast. If that doesn't work,
   surround the sample with aluminum foil.
- Click 'Scan mode' on the console to adjust the focus,
   brightness, contrast and magnification in a smaller portion of
   the picture. Click it again to return to the picture. The focal
   length should be between 6 and 9 mm. Adjust the height (z) to
   achieve this.
- Click 'Acquire' to take the picture (only once or the computer will lock up).
- In the 'Disk' menu, type in the directory, file name (8
   characters max, numbers should be at the end). Then click
   Save and Return in the box. Click 'Save' under 'Image Disk' to
   save the image. The following pictures will be numbered
   consecutively.
- Click 'Live' to take more pictures.

### Change samples:

- Under 'Vacuum Control' click 'Stby' and then 'Vent'
- Insert new sample, shut the door and click 'wet'

 Adjust the height with the z switch until the sample appears to be 0.5 cm from the top

### Shutdown:

- Lower the stage as far as it will go
- Click 'Stby' then 'Vent'
- Under 'Gun' click 'Cool Filament'
- Remove the sample
- Shut the door, wait for the vacuum and then click 'Stby'
- Wait for the filament to reach 0.0A (bottom left corner of the screen)
- Reduce the voltage to zero
- Hit the red button on the console.

## A.9 Flexural Tests

A three-point loading system will be used to determine the flexural modulus of the composite samples. This test can be used to compare the effectiveness of the fiber treatments. An *Instron* 8501-C1002 was used.

- Measure length, width, and thickness of the composite
- Place sample into the testing apparatus
- A support span to depth ratio of 16:1 was used in accordance
   with the ASTM D 790-03 standard
- The composite is bent until it breaks or 5% strain is reached.

• The crosshead speed used was 0.5 in/min, the span was 2.1 in and the loadcell used was 1000 lb

# Appendix B: Electromagnetic Theory

Microwaves range in frequency from 30 MHz to 30 GHz and in wavelength from 1 m to 1 cm. The theory behind microwave interactions with materials is explained in the following sections. Note that vector quantities are shown in bold face type.

# **B.1 Continuity Equation**

The continuity equation is an expression for conservation of charge; charge is constant with time in a closed system.

$$\oint_{S(t)} \mathbf{J}(\mathbf{r},t) \cdot d\mathbf{S} + \int_{V(t)} \frac{\partial \rho(\mathbf{r},t)}{\partial t} = 0$$
(B.1)

J is the electric current density  $(A/m^2)$  and  $\rho$  is the electric charge density  $(C/m^3)$ . The above equation indicates that the current leaving the bounding surface is balanced by the time rate of change of charge density in a volume [129]. This equation can also be written in point (derivative) form.

$$\nabla \cdot \mathbf{J}(\mathbf{r},t) + \frac{\partial \rho(\mathbf{r},t)}{\partial t} = 0$$
 (B.2)

### **B.2 Maxwell's Equations**

Maxwell's equations are fundamental equations governing the behavior of magnetic and electric fields. These equations, in Minkowski form are [129].

$$\nabla \times \mathbf{E}(\mathbf{r},t) = -\frac{\partial \mathbf{B}(\mathbf{r},t)}{\partial t}$$

$$\nabla \times \mathbf{H}(\mathbf{r},t) = \mathbf{J}(\mathbf{r},t) + \frac{\partial \mathbf{D}(\mathbf{r},t)}{\partial t}$$

$$\nabla \cdot \mathbf{D}(\mathbf{r},t) = \rho(\mathbf{r},t)$$

$$\nabla \cdot \mathbf{B}(\mathbf{r},t) = 0$$
(B.3)

where E is the electric field (V/m), B is the magnetic flux density (Wb/m²), H is the magnetic field (A/m), D is the electric displacement (C/m²). The above equations are also called Faraday's law, Ampere's law, Gauss's law and the magnetic Gauss's law respectively. These equations apply at well-behaved or ordinary points where the fields are continuously differentiable. The integral or large-scale forms of Maxwell's equations do not have this restriction [95].

#### **B.3 Constitutive Relations**

Maxwell's equations form an underdetermined system. The additional required equations are called constitutive relations. These equations relate the electromagnetic field quantities and depend on

the properties of the material in which the fields exist. In free space, the constitutive relations are [129]

$$\mathbf{D} = \boldsymbol{\varepsilon}_0 \mathbf{E}$$

$$\mathbf{H} = \frac{1}{\mu_0} \mathbf{B}$$
(B.4)

where  $\varepsilon_0$  is the permittivity of free-space and  $\mu_0$  is the permeability of free space. The form of these constitutive relations changes with the type of material (isotropic, anisotropic, bijsotropic, etc.).

## **B.4 Boundary Conditions**

Boundary conditions are applied where the fields are not continuously differentiable. For a thin, stationary source layer, the boundary conditions are [129]

$$\widehat{n}_{12} \times (\mathbf{H}_1 - \mathbf{H}_2) = J_s$$

$$\widehat{n}_{12} \times (\mathbf{E}_1 - \mathbf{E}_2) = -J_{ms}$$

$$\widehat{n}_{12} \cdot (\mathbf{D}_1 - \mathbf{D}_2) = \rho_s$$

$$\widehat{n}_{12} \cdot (\mathbf{B}_1 - \mathbf{B}_2) = \rho_{ms}$$

$$\widehat{n}_{12} \cdot (\mathbf{J}_1 - \mathbf{J}_2) = -\nabla_s \cdot \mathbf{J}_s - \frac{\partial \rho_s}{\partial t}$$

$$\widehat{n}_{12} \cdot (\mathbf{J}_{m_1} - \mathbf{J}_{m_2}) = -\nabla_s \cdot \mathbf{J}_{ms} - \frac{\partial \rho_{ms}}{\partial t}$$
(B.5)

where  $J_s$  and  $J_{ms}$  are the electric and magnetic currents on the surface. The numbers 1 and 2 represent the two sides of the surface. The boundary conditions on a perfect electric conductor are as follows.

$$\widehat{\boldsymbol{n}} \times \mathbf{H} = \mathbf{J}_{s}$$

$$\widehat{\boldsymbol{n}} \times \mathbf{E} = 0$$

$$\widehat{\boldsymbol{n}} \cdot \mathbf{D} = \rho_{s}$$

$$\widehat{\boldsymbol{n}} \cdot \mathbf{B} = 0$$

$$\widehat{\boldsymbol{n}} \cdot \mathbf{J} = -\nabla_{s} \cdot \mathbf{J}_{s} - \frac{\partial \rho_{s}}{\partial t}$$

$$\widehat{\boldsymbol{n}} \cdot \mathbf{J}_{m} = 0$$
(B.6)

For a perfect magnetic conductor, they are

$$\widehat{\boldsymbol{n}} \times \mathbf{H} = 0$$

$$\widehat{\boldsymbol{n}} \times \mathbf{E} = -\mathbf{J}_{ms}$$

$$\widehat{\boldsymbol{n}} \cdot \mathbf{D} = 0$$

$$\widehat{\boldsymbol{n}} \cdot \mathbf{B} = \rho_{ms}$$

$$\widehat{\boldsymbol{n}} \cdot \mathbf{J}_{m} = -\nabla_{s} \cdot \mathbf{J}_{ms} - \frac{\partial \rho_{ms}}{\partial t}$$

$$\widehat{\boldsymbol{n}} \cdot \mathbf{J} = 0$$
(B.7)

# B.5 TE and TM Modes in a Cylindrical Cavity

The fields in a cylindrical, homogeneous, source free cavity are [95]

$$TM_{z}$$

$$E_{\rho} = \frac{1}{y} \frac{\partial^{2} \psi}{\partial \rho \partial z} \qquad H_{\rho} = \frac{1}{\rho} \frac{\partial \psi}{\partial \phi}$$

$$E_{\phi} = \frac{1}{y \rho} \frac{\partial^{2} \psi}{\partial \phi \partial z} \qquad H_{\phi} = -\frac{\partial \psi}{\partial \rho}$$

$$E_{z} = \frac{1}{y} \left( \frac{\partial^{2}}{\partial z^{2}} + k^{2} \right) \psi \qquad H_{z} = 0$$

$$\begin{split} TE_z \\ E_\rho &= -\frac{1}{\rho} \frac{\partial \psi}{\partial \phi} \qquad H_\rho = \frac{1}{z} \frac{\partial^2 \psi}{\partial \rho \partial z} \\ E_\phi &= \frac{\partial \psi}{\partial \rho} \qquad H_\phi = \frac{1}{z\rho} \frac{\partial^2 \psi}{\partial \phi \partial z} \\ E_z &= 0 \qquad H_z = \frac{1}{z} \left( \frac{\partial^2}{\partial z^2} + k^2 \right) \psi \end{split}$$

$$k = \omega_0 \sqrt{\varepsilon \mu} \tag{B.8}$$

where  $\rho$ ,  $\phi$ , and z are the cylindrical coordinates, and k is the wavenumber. These equations are an expansion of the following equations.

$$TM$$

$$\mathbf{E} = -z\mathbf{u}_{z}\psi + \frac{1}{y}\nabla(\nabla \cdot \mathbf{u}_{z}\psi)$$

$$\mathbf{H} = \nabla \times \mathbf{u}_{z}\psi$$

$$TE$$

$$\mathbf{E} = -\nabla \times \mathbf{u}_{z}\psi$$

$$\mathbf{H} = -y\mathbf{u}_{z}\psi + \frac{1}{z}\nabla(\nabla \cdot \mathbf{u}_{z}\psi)$$
(B.9)

For the derivation, see Harrington [95]. The modes, satisfying PEC boundary conditions are determined by the following equations [95].

$$\psi_{npq}^{TM} = J_n \left( \frac{x_{np} \rho}{a} \right) \sin(n\phi) \cos\left( \frac{q\pi}{d} z \right)$$

$$n, q = 0, 1, 2 \dots$$

$$p = 1, 2, 3 \dots$$

$$\psi_{npq}^{TE} = J_n \left( \frac{x_{np} \rho}{a} \right) \sin(n\phi) \sin\left( \frac{q\pi}{d} z \right)$$

$$n = 0, 1, 2, \dots$$

$$p, q = 1, 2, 3 \dots$$
(B.10)

Where a is the radius and d is the height of the cavity,  $x_{np}$  and  $x_{np}$ ' are the zeros of the Bessel function,  $J_n$ , and its derivative,  $J_n$ '. n indicates the radial periodicity, p is the number of half-wavelengths in the circumferential direction and q is the number of circular wavelengths along the longitudinal axis [78]. These are solutions to the Helmholtz equation.

$$\frac{1}{\rho}\frac{\partial}{\partial\rho}\left(\rho\frac{\partial\psi}{\partial\rho}\right) + \frac{1}{\rho^2}\frac{\partial^2\psi}{\partial\varphi^2} + \frac{\partial^2\psi}{\partialz^2} + k^2\psi = 0 \tag{B.11}$$

 $\Psi$  is a wave function that represents a component of the field.

Figures B1 and B2 show the relationship between the resonant frequency and cavity length of TE and TM modes in an empty cavity with a diameter of 17.78 cm.

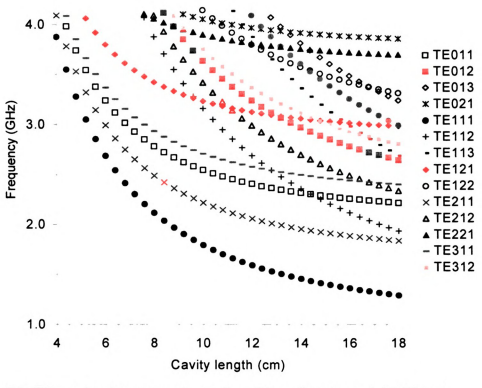


Figure B1: TE modes in an empty cavity with a diameter of 17.78 cm

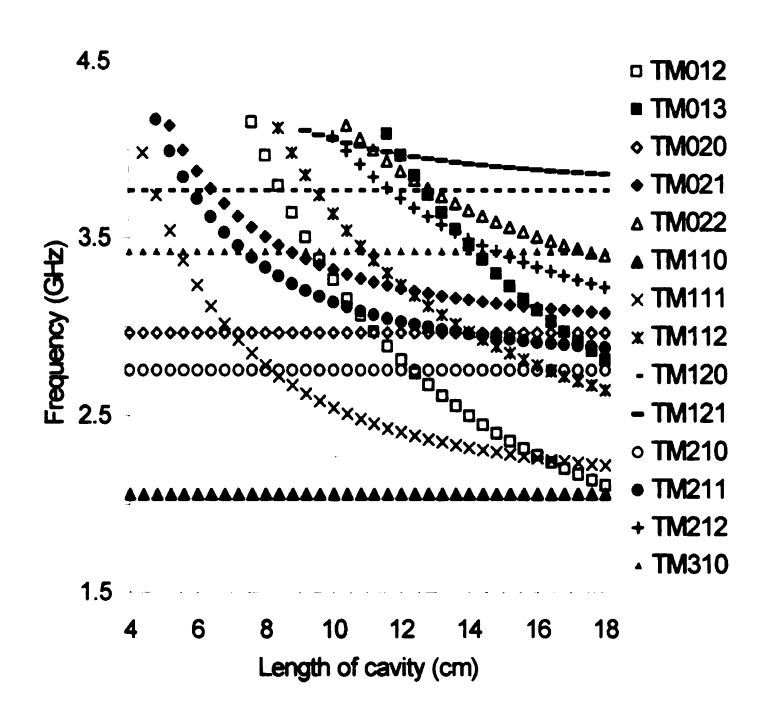


Figure B2: TM modes in an empty cavity with a diameter of 17.78 cm

### **B.6 Material Response to EM Fields**

Materials react differently to electromagnetic fields. For highly conductive materials, most waves will reflect off the surface. The penetration depth of the waves into the material can be described by [78] where  $\omega$  is the frequency,  $\mu_0$  is the permeability of free space,  $\mu$  is the relative permeability and  $\sigma$  is the conductivity.

There are four mechanisms for dielectric polarization: electron (optical), atomic, orientational (dipolar), and interfacial (Figure B1) [78].

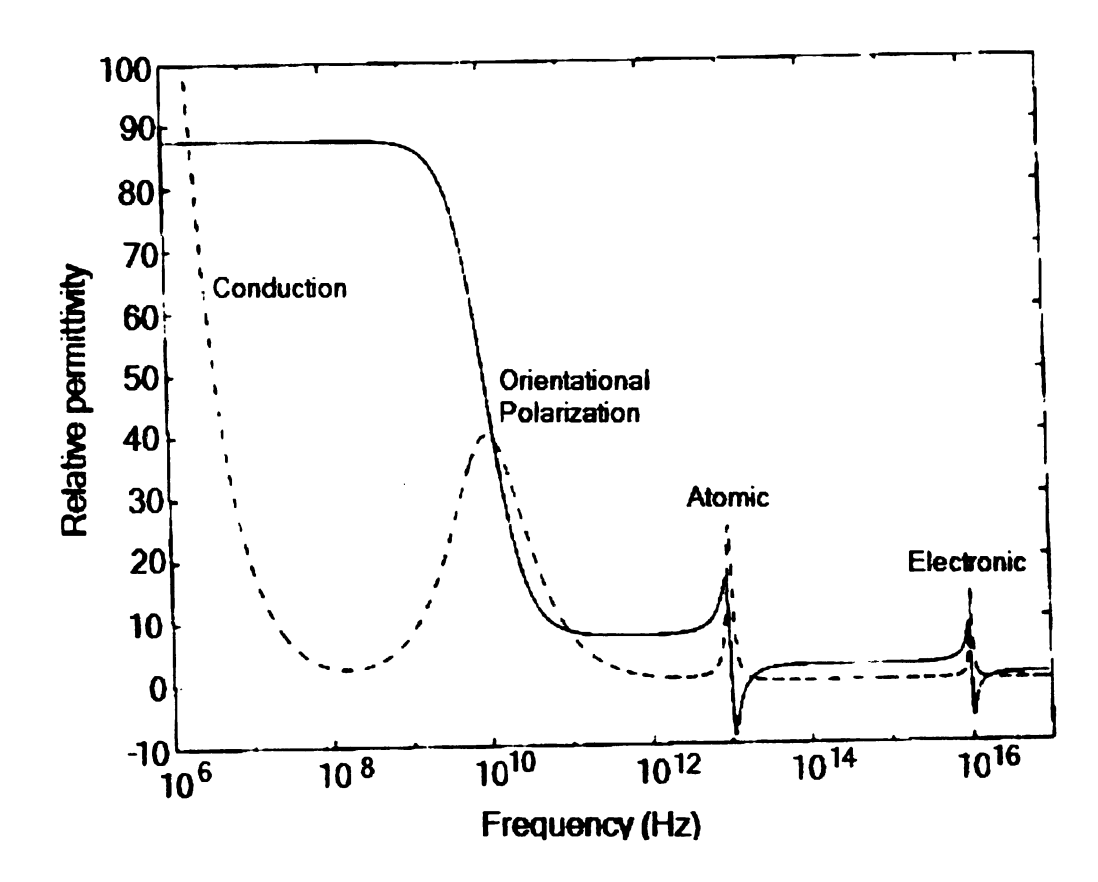


Figure B3: Polarization mechanisms for water. The solid line represents the dielectric constant and the dashed line represents the dielectric loss factor.

Polarization is the distortion of an atom's electron cloud. The time required for polarization to occur is the relaxation time. Electron polarization occurs when the electron cloud of an atom moves in response to an applied electric field. The relaxation time for this mechanism is approximately  $10^{-15}$  s [78]. When atoms within a molecule move relative to each other in response to an electric field it is called atomic polarization. This has a relaxation time of  $10^{-13}$  s [78]. In inhomogeneous materials, charges may accumulate at phase boundaries. These charges can be polarized by an electric

field leading to interfacial polarization. The relaxation time associated with interfacial polarization is on the order of  $10^{-2}$  s for a lignocellulosic fiber reinforced epoxy composite [130]. In dipolar polarization, permanent dipoles rotate to align themselves with the electric field. The relaxation time for dipolar polarization is  $10^{-9}$  s [78]. This mechanism generates heat as friction losses. Since the relaxation time is in the microwave frequency range, and the relaxation time for the other types of polarization are not, dipolar polarization is the mechanism most responsible for microwave heating.

### **B.7 Complex Permittivity**

The complex permittivity describes a material's ability to absorb and store energy.

$$\varepsilon = \varepsilon' - j\varepsilon'' \tag{B.12}$$

The dielectric constant,  $\epsilon'$ , is a measure of energy storage. The dielectric loss factor,  $\epsilon''$ , is a measure of a material's ability to convert stored energy into heat. Generally a high dielectric loss factor,  $\epsilon''$  is needed to heat materials efficiently with microwaves.

### **B.8 Perturbation Method**

The perturbation method uses changes in the cavity Q factor and resonant frequency to calculate the dielectric constant and loss factor of a material. The Q factor is the ratio of frequency multiplied by stored energy to average dissipated power. For a cylindrical cavity and a small cylindrical material the relevant equations are as follows.

$$\frac{\Delta\omega}{\omega} = (\varepsilon' - 1)ABG\frac{V_s}{V_c}$$

$$\frac{1}{Q_s} - \frac{1}{Q_0} = 2\varepsilon''ABG\frac{V_s}{V_c}$$
(B.13)

$$A = J_0 \left(\frac{2.405R_s}{R_c}\right)^2 + J_1 \left(\frac{2.405R_s}{R_c}\right)^2$$

$$B = 1 + \left(\frac{L_c}{2\pi L_s}\right) \sin\left(\frac{2\pi L_s}{L_c}\right)$$

$$G = 0.2718 \left(\frac{\omega_0}{\omega_0 R_c}\right)^2$$

$$\Delta \omega = \omega_0 - \omega_s$$
(B.14)

Where  $\epsilon'$  is the permittivity,  $\epsilon''$  is the loss factor,  $\omega_0$ ,  $Q_0$ ,  $R_c$ ,  $L_c$ ,  $V_c$  are the unloaded cavity resonant frequency, quality factor, radius, length and volume. The loaded cavity resonant frequency and quality factors are  $\omega_s$  and  $Q_s$  [131]. Q is equal to the resonant

frequency divided by the change in frequency at the half-power point (Figure B2).

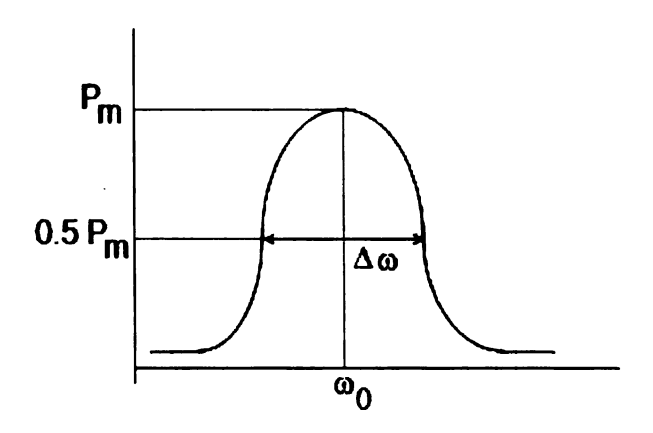


Figure B4: Absorbed power vs. frequency plot.

The swept-frequency method is used to determine the cavity length, empty and loaded cavity resonant frequencies, and half-power bandwidth necessary to calculate the dielectric properties. For these equations to apply, the resonant frequency change must be small  $(\Delta\omega/\omega_0 < 1\%)$  [131].

**REFERENCES** 

- Mohanty, A.K., M. Misra, and G. Hinrichsen, Biofibres, biodegradable polymers and biocomposites: An overview.
   Macromolecular Materials and Engineering, 2000. 276/277: p. 1 24.
- 2. Handbook of Fiber Chemistry. International Fiber Science and Technology Series, ed. M. Lewin and E.M. Pearce. Vol. 15. 1998, New York: Marcel Dekker, Inc. 1083.
- 3. Li, X., L.G. Tabil, and S. Panigrahi, Fiber-Reinforced Composites: A Review. Journal of Polymers and the Environment, 2007. In Press.
- 4. Sherman, L.M., Natural Fibers: The New Fashion in Automotive Plastics. Plastics Technology, 1999. 45(10): p. 62-68.
- 5. Sydenstricker, T.H., S. Mochnaz, and S.C. Amico, *Pull-out and other evaluations in sisal-reinforced polyester biocomposites*. Polymer Testing, 2003. **22**(4): p. 375-380.
- 6. Manikandan, K.C., S.M. Diwan, and S. Thomas, Tensile Properties of Short Sisal Fiber Reinforced Polystyrene Composites. Journal of Applied Polymer Science, 1996. 60: p. 1483 1497.
- 7. Eichhorn, S.J., et al., Current international research into cellulosic fibres and composites. Journal of Materials Science, 2001. 39(9): p. 2107-2131.
- 8. Maldas, D., et al., Improvement of the mechanical properties of sawdust wood fibre-polystyrene composites by chemical treatment. Polymer, 1988. 29(7): p. 1255-1265.
- 9. Toriz, G., F. Denes, and R.A. Young, Lignin-Polypropylene Composites. Part 1: Composites From Unmodified Lignin and Polypropylene. Polymer Composites, 2002. 23(5): p. 806 811.
- Karnani, R., M. Krishnan, and R. Narayan, Biofiber-Reinforced Polypropylene Composites. Polymer Engineering and Science, 1997.
   37(2): p. 476 482.

- 11. Pavithran, C., et al., Copper coating on coir fibres. Journal of Materials Science, 1981. 16: p. 1548 1556.
- 12. Man-Made Fibers Science and Technology, ed. H.F. Mark, S.M. Atlas, and E. Cernia. Vol. 3. 1968: Interscience Publishers. 706.
- 13. Wambua, P., J. Ivens, and I. Verpoest, *Natural fibres: can they replace glass in fibre reinforced plastics?* Composites Science and Technology, 2003. **63**: p. 1259 1264.
- 14. Shin, C., Filtration application from recycled expanded polystyrene. Journal of Colloid and Interface Science, 2006. 302: p. 267 271.
- 15. Knefelkamp, B., K. Carstens, and K.H. Wiltshire, Comparison of different filter types on chlorophyll-a retention and nutrient measurements. Journal of Experimental Marine Biology and Ecology, 2007. 345: p. 61 70.
- 16. Park, E.-S., Mechanical Properties and Processibilty of Glass-Fiber-, Wollastonite-, and Fluoro-Rubber-Reinforced Silicone Rubber Composites. Journal of Applied Polymer Science, 2007. 105: p. 460 468.
- 17. Manchado, M.A. and M. Arroyo, Short Fibers as Reinforcement of Rubber Compounds. Polymer Composites, 2002. 23(4): p. 666 673.
- 18. Karacaer, O., et al., Dynamic Mechanical Properties of Dental Base Material Reinforced with Glass Fiber. Journal of Applied Polymer Science, 2002. 85: p. 1683 1697.
- 19. Kennedy, K.C., T. Chen, and R.P. Kusy, Behavior of photopolymerized silicate-glass-fibre-reinforced dimethacrylate composites subjected to hydrothermal ageing: Part II Hydrolytic stability of mechanical properties. Journal of Materials Science: Materials in Medicine, 1998. 9: p. 651 660.
- 20. Kanie, T., et al., Flexural properties and impact strength of denture base polymer reinforced with woven glass fibers. Dental materials, 2000. 16: p. 150 158.

- 21. Miettinen, V.M. and P.K. Vallittu, Release of residual methyl methacrylate into water from glass fibre-poly(methyl methacrylate) composite used in dentures. Biomaterials, 1997. 18(2): p. 181 185.
- 22. Vallittu, P.K., V.P. Lassila, and R. Lappalainen, Transverse strength and fatigue of denture acrylic-glass fiber composite. Dental Materials, 1994. 10: p. 116 121.
- 23. Fitch, P.E. and J.S. Cooper, Life Cycle Energy Analysis as a Method for Material Selection. Transactions of the ASME, 2004. 126: p. 798 804.
- 24. Mohanty, S. and Y.P. Chugh, Development of fly ash-based automotive brake lining. Tribology International, 2007. 40: p. 1217 1224.
- 25. Lee, N.-J. and J. Jang, The effect of fibre content on the mechanical properties of glass fibre mat/polypropylene composites.

  Composites: Part A, 1999. 30: p. 815 822.
- 26. Dahlke, B., et al., Natural Fiber Reinforced Foams Based on Renewable Resources for Automotive Interior Applications. Journal of Cellular Plastics, 1998. 34: p. 361 379.
- 27. Fraga, A.N., et al., Relationship between Water Absorption and Dielectric Behavior of Glass Fiber Reinforced Unsaturated Polyester Resin. Journal of Composite Materials, 2006. 41(4): p. 393 402.
- 28. Joseph, K., et al., Influence of Interfacial Adhesion on the Mechanical Properties and Fracture Behavior of Short Sisal Fiber Reinforced Polymer Composites. European Polymer Journal, 1996. 32(10): p. 1243 1250.
- 29. Bisanda, E.T.N. and M.P. Ansell, The Effect of Silane Treatment on the Mechanical and Physical Properties of Sisal-Epoxy Composites. Composites Science and Technology, 1991. 41(2): p. 165-178.
- 30. Mishra, S., et al., Potentiality of Pineapple Leaf Fibre as Reinforcement in PALF-Polyester Composite: Surface Modification

- and Mechanical Performance. Journal of Reinforced Plastics and Composites, 2001. 20(4): p. 321-334.
- 31. Rout, J., et al., Novel Eco-Friendly Biodegradable Coir-Polyester Amide Biocomposites: Fabrication and Properties Evaluation. Polymer Composites, 2001. 22(6): p. 770 778.
- 32. Gulati, D. and M. Sain, Surface Characteristics of Untreated and Modified Hemp Fibers. Polymer Engineering and Science, 2006. 46(3): p. 269 273.
- 33. Mehta, G., et al., Effect of Fiber Surface Treatment on the Properties of Biocomposites from Nonwoven Industrial Hemp Fiber Mats and Unsaturated Polyester Resin. Journal of Applied Polymer Science, 2005. 99: p. 1055 1068.
- 34. Shanks, R.A., A. Hodzic, and D. Ridderhof, Composites of Poly(lactic acid) with Flax Fibers Modified by Interstitial Polymerization. Journal of Applied Polymer Science, 2005. 99: p. 2305 2313.
- 35. Mishra, S., et al., Novel Eco-Friendly Biocomposites: Biofiber Reinforced Biodegradable Polyester Amide Composites-Fabrication and Properties Evaluation. Journal of Reinforced Plastics and Composites, 2002. 21(1): p. 55-70.
- 36. Mishra, S., et al., The Influence of Chemical Surface Modification on the Performance of Sisal-Polyester Biocomposites. Polymer Composites, 2002. 23(2): p. 164 170.
- 37. Kokta, B.V., et al., Composites of Polyvinyl Chloride-Wood Fibers.

  I. Effect of Isocyanate as a Bonding Agent. Polymer-Plastics
  Technology and Engineering, 1990. 29(1&2): p. 87-118.
- 38. Arbelaiz, A., et al., Thermal and crystallization studies of short flax fibre reinforced polypropylene matrix composites: Effect of treatments. Thermochimica Acta, 2005. 440: p. 111 121.
- 39. Rodriguez, E.S., P.M. Stefani, and A. Vazquez, Effects of Fibers' Alkali Treatment on the Resin Transfer Molding Processing and

- Mechanical Properties of Jute-Vinylester Composites. Journal of Composite Materials, 2007. 41(14): p. 1729 1741.
- 40. Pickering, K.L., et al., Optimising industrial hemp fibre for composites. Composites: Part A, 2007. 38: p. 461 468.
- 41. Goda, K., et al., Improvement of plant based natural fibers for toughening green composites—Effect of load application during mercerization of ramie fibers. Composites: Part A, 2006. 37: p. 2213 2220.
- 42. Abdelmouleh, M., et al., Short natural-fibre reinforced polyethylene and natural rubber composites: Effect of silane coupling agents and fibres loading. Composites Science and Technology, 2007. 67: p. 1627 1639.
- 43. Huda, M.S., et al., The effect of silane treated- and untreated-talc on the mechanical and physico-mechanical properties of poly(lactic acid)/newspaper fibers/talc hybrid composites. Composites: Part B, 2007. 38: p. 367 379.
- 44. Tripathy, P.C., et al., Studies of Cu(II)-IO4- initiated graft copolymerization of methyl methacrylate from defatted pineapple leaf fibres. Polymer International, 1999. 48: p. 868 872.
- 45. Mohanty, A.K., S. Parija, and S. Mishra, Ce(1V)-N-Acetylglycine Initiated Graft Copolymerization of Acrylonitrile onto Chemically Modified Pineapple Leaf Fibers. Journal of Applied Polymer Science, 1996. **60**: p. 931 937.
- 46. DiBenedetto, A.T., Tailoring of interfaces in glass fiber reinforced polymer composites: a review. Materials Science and Engineering, 2001. A302: p. 74 82.
- 47. Fujihara, K., et al., Fibrous composite materials in dentistry and orthopaedics: review and applications. Composites Science and Technology, 2004. 64: p. 775 788.

- 48. Meric, G. and I.E. Ruyter, Effect of thermal cycling on composites reinforced with two differently sized silica-glass fibers. Dental Materials, 2007. 23: p. 1157 1163.
- 49. Jancar, J., Hydrolytic stability of PC/GF composites with engineered interphase of varying elastic modulus. Composites Science and Technology, 2006. 66: p. 3144 3152.
- 50. Felix, A.H.O., et al., Influence of Reactice Processing on the Properties of PP/Glass Fiber Composites Compatibilized with Silane. Macromolecular Materials and Engineering, 2006. 291: p. 418 427.
- 51. Jensen, R.E. and S.H. McKnight, Inorganic-organic fiber sizings for enhanced energy absorption in glass fiber-reinforced composites intended for structural applications. Composites Science and Technology, 2006. 66: p. 509 521.
- 52. Pavlidou, S., K. Krassa, and C.D. Papaspyrides, Woven Glass Fabric/Polyester Composites: Effect of Interface Tailoring on Water Absorption. Journal of Applied Polymer Science, 2005. 98: p. 843 851.
- 53. DiBenedetto, A.T., et al., Reactive coupling of fibers to engineering thermoplastics. Composite Structures, 1994. 27: p. 73 82.
- 54. Gao, S.L., E. Mader, and R. Plonka, Nanostructured coatings of glass fibers: Improvement of alkali resistance and mechanical properties. Acta Materialia, 2007. 55: p. 1043 1052.
- 55. Barazza, H.J., et al., Moisture absorption and wet-adhesion properties of resin transfer molded (RTM) composites containing elastomer-coated glass fibers. Journal of Adhesion Science and Technology, 2003. 17(2): p. 217 242.
- 56. Tanoglu, M., et al., The effects of glass-fiber sizings on the strength and energy absorption of the fiber/matrix interphase under high loading rates. Composites Science and Technology, 2001. 61: p. 205 220.

- 57. O'Brien, R.N. and K. Hartman, Air Infrared Spectroscopy Study of the Epoxy-Cellulose Interface. Journal of Polymer Science: Part C, 1971. 34: p. 293 301.
- 58. Datta, C., D. Basu, and A. Banerjee, Mechanical and Dynamic Mechanical Properties of Jute Fibers-Novolac-Epoxy Composite Laminates. Journal of Applied Polymer Science, 2002. 85: p. 2800 2807.
- 59. Rong, M.Z., et al., The effect of fiber treatment on the mechanical properties of unidirectional sisal-reinforced epoxy composites.

  Composites Science and Technology, 2001. 61: p. 1437 1447.
- 60. Oskman, K., High Quality Flax Fibre Composites Manufactured by the Resin Transfer Moulding Process. Journal of Reinforced Plastics and Composites, 2001. 20(7): p. 621-627.
- 61. Rajulu, A.V., et al., Chemical Resistance and Tensile Properties of Short Bamboo Fiber Reinforced Epoxy Composites. Journal of Reinforced Plastics and Composites, 1998. 17(7): p. 1507-1511.
- 62. Patel, R.H. and R.G. Patel, Studies on the properties of glass fiber reinforced epoxy composites of DGEBA / epoxidized polyhydric alcohols with or without fortifier Die Angewandte Makromolekulare Chemie, 1990. 181: p. 75-84.
- 63. Kraynak, C., E. Akgul, and N.A. Isitman, Effects of RTM Mold Temperature and Vacuum on the Mechanical Properties of Epoxy/Glass Fiber Composite Plates. Journal of Composite Materials, 2008. 42(15): p. 1505-1521.
- 64. Lee, W.I. and G.S. Springer, Interaction of Electromagnetic Radiation with Organic Matrix Composites. Journal of Composite Materials, 1984. 18: p. 357-386.
- 65. Abdel-Magid, B., et al., The combined effects of load, moisture and temperature on the properties of E-glass/epoxy composites.

  Composite Structures, 2005. 71: p. 320-326.

- 66. George, C.E., G.R. Lightsey, and A.G. Wehr, Materials Research Society Symposium Proceedings. 1988. Microwave Processing of Materials.
- 67. Hottong, U., et al., Ceramic Transactions, 1991. 21: p. 587.
- 68. Jullien, H. and H. Valot, Polymer, 1985. 26: p. 505.
- 69. Lewis, D.A., et al., Journal of Polymer Science: Part A: Polymer Chemistry,, 1992. 30: p. 1647
- 70. Jow, J., Microwave Processing and Dielectric Diagnosis of Polymers and Composites using a Single-Mode Resonant Cavity Technique, in Chemical Engineering. 1988, Michigan State University: East Lansing.
- 71. Wei, J., M.C. Hawley, and M.T. Demeuse, Kinetics modeling and time-temperature-transformation diagram of microwave and thermal cure of epoxy resins. Polymer Engineering and Science, 1995. 35(6): p. 461.
- 72. Wei, J., Microwave processing of epoxy resins and graphite fiber/epoxy composites in a cylindrical tunable resonant cavity, in Chemical Engineering. 1992, Michigan State University: East Lansing.
- 73. Wei, J., et al., Polymer Engineering and Science, 1993(33): p. 1132.
- 74. Agrawal, R. and L.T. Drzal, Journal of Adhesion, 1989. 29: p. 63.
- 75. Paulauskas, F.L., T.T. Meek, and C.D. Warren. MRS Symposium Proceedings. 1996.
- 76. Wei, J., F.L. Paulauskas, and W.G. Johanson, Industrial Processing Via Variable Frequency Microwaves. Part I: Bonding Applications. 1998.

- 77. Fellows, L.A., R. Delgado, and M.C. Hawley. in 26th International SAMPE Technical Conference. 1994. Atlanta, GA.
- 78. Qiu, Y., Variable Frequency Microwave Processing and Microwave Process Control for Polymer Composites, in Chemical Engineering. 2000, Michigan State University: East Lansing.
- 79. Zhou, S., Interactions in microwave adhesive bonding of polymers and composites, in Chemical Engineering and Materials Science. 2002, Michigan State University: East Lansing. p. 202.
- 80. Zong, L., MICROWAVE PROCESSING OF EPOXY RESINS AND SYNTHESIS OF CARBON NANOTUBES BY MICROWAVE PLASMA CHEMICAL VAPOR DEPOSITION, in Chemical Engineering and Materials Science. 2005, Michigan State University: East Lansing, MI. p. 189.
- 81. Pracella, M., et al., Functionalization, compatibilization and properties of polypropylene composites with Hemp fibres.

  Composites Science and Technology, 2006. 66: p. 2218-2230.
- 82. Choi, J.S., et al., Rheological, Thermal, and Morphological Characteristics of Plasticized Cellulose Acetate Composite with Natural Fibers. Macromolecular Symposium, 2005. 224: p. 297-307.
- 83. Biagiotti, J., et al., A Systematic Investigation on the Influence of the Chemical Treatment of Natural Fibers on the Properties of Their Polymer Matrix Composites. Polymer Composites, 2004. 25(5): p. 470 479.
- 84. Liu, W., et al., Effects of alkali treatment on the structure, morphology and thermal properties of native grass fibers as reinforcements for polymer matrix composites. Journal of Materials Science, 2004. 39: p. 1051 1054.
- 85. Mwaikambo, L.Y. and M.P. Ansell, Chemical Modification of Hemp, Sisal, Jute, and Kapok Fibers by Alkalization. Journal of Applied Polymer Science, 2002. 84: p. 2222 2234.

- 86. Khan, M.A. and L.T. Drzal, Characterization of 2-hydroxyethyl methacrylate (HEMA)-treated jute surface cured by UV radiation. Journal of Adhesion Science and Technology, 2004. 18(3): p. 381-393.
- 87. Zafeiropoulos, N., P.E. Vickers, and C.A. Baillie, An experimental investigation of modified and unmodified flax fibres with XPS, ToF-SIMS and ATR-FTIR. Journal of Materials Science, 2003. 38: p. 3903 3914.
- 88. Tserki, V., et al., Development of Biodegradable Composites with Treated and Compatibilized Lignocellulosic Fibers. Journal of Applied Polymer Science, 2006. 100: p. 4703 4710.
- 89. Olmos, D., R. Lopez-Moron, and J. Gonzalez-Benito, The nature of the glass fibre surface and its effect in the water absorption of glass fibre/epoxy composites. The use of fluorescence to obtain information at the interface. Composites Science and Technology, 2006. 66(15): p. 2758 2768.
- 90. Williams, G.I. and R.P. Wool, Composites from Natural Fibers and Soy Oil Resins. Applied Composite Materials, 2000. 7: p. 421 432.
- 91. Tajvidi, M., S.K. Najafi, and N. Moteei, Long-Term Water Uptake Behavior of Natural Fiber/Polypropylene Composites. Journal of Applied Polymer Science, 2005. 99: p. 2199 2203.
- 92. Natural Fibers, Biopolymers, and Biocomposites, ed. A.K. Mohanty, M. Misra, and L.T. Drzal. 2005, Boca Raton: CRC Press. 875.
- 93. Huang, X. and A. Netravali, Characterization of flax fiber reinforced soy protein resin based green composites modified with nano-clay particles. Composites Science and Technology, 2007. 67(10): p. 2005 2014.
- 94. Dow-Corning. Z-6040 Silane. Product Information: Organofunctional Silanes 2005 10/7/2005 [cited 2007 11/10].

- 95. Harrington, R.F., Time-Harmonic Electromagnetic Fields. 2001: IEEE Press.
- 96. Rowell, R.M., J.S. Han, and J.S. Rowell, Characterization and Factors Effecting Fiber Properties, in Natural polymers and agrofibers based composites: preparation, properties and applications, E. Frollini, A.L. Leão, and L.H.C. Mattoso, Editors. 2000, L.H.C., Embrapa: San Carlos, Brazil. p. 115 134.
- 97. Rymsza, T.A., Kenaf and Hemp: Identifying the Differences, in American Kenaf Society. 2000: Corpus Christi, Texas.
- 98. Ganan, P., et al., Stem and Bunch Banana Fibers from Cultivation Wastes: Effect of Treatments on Physico-Chemical Behavior.

  Journal of Applied Polymer Science, 2004. 94: p. 1489 1495.
- 99. Tserki, V., et al., A study of the effect of acetylation and propionylation surface treatments on natural fibres. Composites: Part A, 2005. 36: p. 1110 1118.
- 100. Garside, P. and P. Wyeth, Identification of cellulosic fibres by FTIR spectroscopy: thread and single fibre analysis by attenuated total reflectance. Studies in Conservation, 2003. 48: p. 269 275.
- 101. Lee, H. and N. K, Epoxy Resins: Their Applications and Technology. 1957, New York: McGraw-Hill.
- 102. Finzel, M., in *Chemical Engineering*. 1991, Michigan State University: East Lansing.
- Yousefi, A., P.G. Lafleur, and R. Gauvin, Kinetic Studies of Thermoset Cure Reactions: A Review. Polymer Composites, 1997. 18(2): p. 157 - 168.
- 104. Prime, B., Thermal Characterization of Polymeric Materials. 1981: Academic Press.

- 105. Acitelli, M.A., R.B. Prime, and E. Sacher, Kinetics of epoxy cure: (1) The system bisphenol-A diglycidyl ether/m-phenylene diamine Polymer, 1971. 12: p. 335 343.
- 106. Kamal, M.R., Thermoset Characterization for Moldability Analysis. Polymer Engineering and Science, 1974. 14(3): p. 231 239.
- 107. Kamal, M.R. and S. Sourour, Kinetics and Thermal Characterization of Thermoset Cure. Polymer Engineering and Science, 1973. 13: p. 59 64.
- 108. Chan, A.W. and S.T. Hwang, Modeling of the Impregnation Process During Resin Transfer Molding. Polymer Engineering and Science, 1991. 31: p. 1149 1156.
- 109. Fu, B. and M.C. Hawley, Comparative Study of Continuous-Power and Pulsed-Power Microwave Curing of Epoxy Resins. Polymer Engineering and Science, 2000. 40(10): p. 2133 2143.
- 110. Holbery, J. and D. Houston, Natural-Fiber-Reinforced Polymer Composites in Automotive Applications. JOM, 2006. 58(11): p. 80-87.
- 111. Herrmann, A.S., J. Nickel, and U. Riedel, Construction materials based upon biologically renewable resources-from components to finished parts. Polymer Degradation and Stability, 1998. 59: p. 251-261.
- 112. Arora, S., Biodegradability of Biobased Composites, in Chemical Engineering and Materials Science. 2006, Michigan State University: East Lansing, Mi. p. 293.
- 113. Kaldor, A.K., Kenaf, an alternative fiber for the pulp and paper industries in developing and developed countries. Tappi, 1992. 75(10): p. 141 145.
- 114. Pellegrino, J.L., Energy and Environmental Profile of the U.S. Glass Industry. 2002, U.S. Department of Energy: Columbia, Maryland.

- 115. Bismarck, A., A. Baltazar-y-Jimenez, and K. Sarikakis, Green Composites as Panacea? Socio-Economic Aspects of Green Materials. Environment, Development and Sustainability, 2006. 8: p. 445 463.
- 116. Thostenson, E.T. and T.W. Chou, *Microwave processing:* fundamentals and applications. Composites: Part A, 1999. 30: p. 1055 1071.
- 117. Boey, F., I. Gosling, and S.W. Lye, *High-pressure microwave curing process for an epoxy-matrix/glass-fibre composite*. Journal of Materials Processing Technology, 1992. **29**: p. 311 319.
- 118. Feher, L., M. Thumm, and K. Drechsler, Gigahertz and Nanotubes Perspectives for Innovations withNovel IndustrialMicrowave Processing Technology. Advanced Engineering Materials, 2006. 8(1-2): p. 26 32.
- 119. Sparnins, E., Mechanical properties of flax fibers and their composites, in Department of Applied Physics and Mechanical Engineering. 2006, Lulea University of Technology: Lulea, Sweden. p. 84.
- 120. Burgueno, R., et al., Sustainable Cellular Biocomposites from Natural Fibers and Unsaturated Polyester Resin for Housing Panel Applications. Journal of Polymers and the Environment, 2005. 13(2): p. 139 149.
- 121. Arib, R.M.N., et al., Mechanical properties of pineapple leaf fibre reinforced polypropylene composites. Materials and Design, 2006. 27: p. 391 396.
- 122. Luo, S. and A.N. Netravali, Characterization of henequen fibers and the henequen fiber/poly(hydroxybutyrate-co-hydroxyvalerate) interface. Journal of Adhesion Science and Technology, 2001. 15(4): p. 423 437.
- 123. Shaikh, A.A. and S.A. Channiwala, Strength Prediction for Jute Polyester Composite for Transverse Fiber Reinforcement. Material Science Forum, 2007. 561 565: p. 799 802.

- 124. Sun, R., Electromagnetic Modeling of an Adaptable Multimode Microwave Applicator for Polymer Processing. Applied Computational Electromagnetic Society, 2005. 20(1): p. 43 49.
- 125. Haines, P.J., ed. Principles of Thermal Analysis and Calorimetry. 2002, Royal Society of Chemistry.
- 126. Griffiths, P.R., Fourier Transform Infrared Spectrometry (Chemical Analysis: A Series of Monographs on Analytical Chemistry and Its Applications). 2007: Wiley-Interscience.
- 127. Barr, T., L., Modern ESCA: The Principles and Practice of X-Ray Photoelectron Spectroscopy. 1994: CRC.
- 128. Heckman, J.W., K.L. Klomparens, and S.L. Flegler, Scanning and Transmission Electron Microscopy: An Introduction. 1993: Oxford University Press.
- 129. Rothwell, E.J. and M.J. Cloud, Electromagnetics. 2001: CRC Press.
- 130. Arous, M., et al., Experimental Study on Dielectric Relaxation in Alfa Fiber Reinforced Epoxy Composites. Journal of Applied Polymer Science, 2007. 106: p. 3631-3640.
- 131. Jow, J., et al., Microwave Processing and Diagnosis of Chemically Reacting Materials in a Single-Mode Cavity Applicator. IEEE Transactions on Microwave Theory and Techniques, 1987. MTT-35(12): p. 1435 1433.

